Version of Record: https://www.sciencedirect.com/science/article/pii/S0025322720302085
Manuscript_1ddd8a964e6e74e0d6f6df9bdffbcf15

Carbonate crusts around volcanic islands: composition, origin and their significance in slope stability

Maurice E. Tucker[1], Steven N. Carey[2], R. Stephen J. Sparks[1], Adam Stinton[3,4], Melanie Leng[5], Laura Robinson[1], Tao Li[1,6], Jamie Lewis[1], Laura Cotton[1,7]

1. School of Earth Sciences, University of Bristol, Bristol BS8 1RJ, UK
2. Graduate School of Oceanography, University of Rhode Island, Narragansett, R.I. 02882
3. Montserrat Volcano Observatory, PO Box 316, Fleming, MSR 1110, Montserrat
4. Seismic Research Centre, The University of the West Indies, St Augustine, Trinidad and Tobago
5. British Geological Survey, Keyworth, Nottingham NG12 5GG, UK and School of Biosciences, University of Nottingham, Sutton Bonington Campus, Loughborough LE12 5RD, UK
6. Department of Earth and Planetary Sciences, Nanjing University, 163 Xianlin Road, Nanjing 210023, China
7. School of Earth & Environmental Sciences, University of Portsmouth, Burnaby Building, Burnaby Road, Portsmouth PO1 3QL, UK

ABSTRACT

Extensive carbonate crusts discovered forming on the slopes of seamounts in many parts of the world's oceans are providing extra stability to the volcanic edifices. These crusts are hardgrounds composed of mixtures of volcaniclastic debris and bioclastic material, in most cases cemented by calcite, in the form of isopachous coatings around grains and pore-filling spar. Such crusts, which have been collected by a remotely-operated vehicle (ROV), are described here from moderate-depth to deeper-water slopes (180 – 820 m) around the volcanic island of Montserrat in the Caribbean, and from the nearby Kick'em Jenny submarine volcano off Grenada. Radiogenic $^{87}Sr/^{86}Sr$ isotope ratios from the carbonates give an indication of age (up to 0.4 Ma years old) but they also demonstrate that some samples have been altered by hydrothermal-volcanic processes, to give ages much older than expected (14 to 18 Ma) based on the foraminifera present. Such alteration is also supported by carbon and oxygen isotope ($\delta^{13}C$ and $\delta^{18}O$) ratios, although most samples retain typical marine values. In many cases $\delta^{18}O$ is usually a little more positive than expected from modern Caribbean shallow-water carbonates, likely reflecting cooler water at their moderate depths of lithification. Just one sample, from Kick'em Jenny, has very negative $\delta^{13}C$ (-42 ‰) indicating methanogenesis. Crusts are also reported here from the Mediterranean Sea, with an example described from Kolumbo submarine volcano, northeast of the Santorini volcanic complex in the Hellenic subduction zone, that are similar in many respects to those from the Caribbean. Typically, the biota of the crusts consists of calcareous red algae (commonly

encrusting volcanic clasts), foraminifera (benthic, some also encrusting, and planktic), subordinate serpulids, bivalves, pteropods and heteropods, and rare deeper-water corals. Some bioclasts are derived from shallower water, others from the moderate depths of the slope itself, and planktic fallout. In addition, there is evidence for the former presence of microbes from the occurrence of calcified filaments and peloids in intragranular cavities. Several generations of sponge borings are usually present as well as calcite cement. Dissolution and calcite replacement of aragonitic bioclasts and cement, and sponge spicules (originally opaline silica), have taken place. The carbonate crusts are attributed to seawater circulating within the surficial sediment, in some cases mixing with hydrothermal fluid driven by geothermal and volcanic processes. Submarine volcanic slopes clearly provide a location for moderate-depth carbonate production and cementation, but a further significance of these hardgrounds is in stabilising seamounts, enabling their slopes to avoid frequent collapse, dissection and readjustment. However, when failure does occur, larger-scale submarine landslides involving coherent slabs are more likely.

Keywords: Seamounts, Montserrat, hardgrounds, carbonate crusts, slope crusts,

1. Introduction

Volcanic islands are favourable environments for the formation of carbonate sediment. Much attention has focussed on the formation of coral islands and atolls by the subsidence of volcanic edifices following on from Darwin's seminal work (Darwin, 1874; Stoddart, 1976). Coral reefs surround volcanic islands and protect them from erosion by waves and storms. They are generated by biological activity but cementation is also involved due to interaction with carbonate-saturated fluids, notably seawater. In some cases these coral reefs, once in shallow-water, now occur on the flanks of seamounts as a result of major subsidence; several such terraces are recorded depths down to 1000 m on Hawaii (Moore and Fornari, 1984; Webster et al., 2009). By way of contrast, we have discovered extensive carbonate-cemented crusts that mantle and armour the deeper flanks of volcanic islands and seamounts as submarine hardgrounds to water depths of nearly 1000 m. The hardgrounds form by cementation of volcaniclastic and bioclastic deposits that drape seamount slopes. Although hardgrounds are relatively common in shallow-water successions throughout the geological record, but are relatively rare in deeper-water facies (Christie et al., 2015), the term "hardground" was first introduced by Murray and Renard (1891) as a descriptive term for

rocky seafloors in the deep-sea discovered during the voyage of HMS Challenger in 1872-6. 'Classic' modern-Quaternary shallow-water hardgrounds are well-documented from carbonate-dominated locations such as the Bahamas and Arabian Gulf (e.g. Shinn, 1968; Dravis, 1978) and deeper-water ones occur there on slopes too (e.g. Schlager and James, 1978; Malone et al., 2001), as well as in the Mediterranean (Allouc, 1990; Aghib et al., 1991) and on cold-water mound structures, such as Porcupine Bank, in the NE Atlantic (Noé et al., 2006; van der Land et al., 2010). There are, however, few reports of carbonate crusts on the slopes of seamounts and volcanic ridges, apart from some documented from the Mid-Atlantic Ridge (Thompson et al., 1968; Schroeder et al., 2002), the Mediterranean (McKenzie and Bernoulli, 1982) and Red Sea (e.g., Milliman, 1974). Some Quaternary hardgrounds have been related to sea-level and climate changes (see reviews of van der Kooij et al., 2010 and Christ et al., 2015).

Exploration of the submarine flanks of active volcanoes and volcanic seamounts during expeditions of the EV *Nautilus* has revealed common limestone crusts (hardgrounds) covering their submarine slopes, with unlithified sediment below. These crusts typically consist of volcanogenic clastic and biogenic material cemented by calcite coating the slopes and extending to water depths of several 100 to nearly a 1000 metres. They vary from several tens of centimetres to a few metres thick and form distinctive slabs when fractured. They have been observed on the submarine slopes of the Soufrière Hills Volcano, Montserrat in the Eastern Caribbean, and around several seamounts and young submarine volcanoes in the Mediterranean and in the Galapagos Islands, all of which have been sampled.

To our knowledge such carbonate crusts on seamount slopes have not been widely recognised or described. However, they are significant from several perspectives. First, they represent a new location of limestone deposition in the world's oceans. Second, the hardgrounds act to protect the submarine flanks of volcanic islands and seamounts from erosion and collapse and they may inhibit submarine intrusion of seawater into the interior of such volcanic edifices. In addition, they also form important hard substrates for the development of benthic biological communities.

This study focuses on the development of limestone crusts with a case study of the Soufrière Hills Volcano (SHV), Montserrat, together with descriptions of occurrences on other seamounts, in the southern Lesser Antilles (Kick'em Jenny submarine volcano) and, as a Mediterranean example, the Kolumbo seamounts from the Hellenic Arc in the Aegean Sea. We also note limestones sampled on Montserrat, at outcrop and in geothermal boreholes and as clasts in debris-avalanche deposits since they are pertinent to understanding the role of

hydrothermal and ground-water systems in forming the limestone crusts. The origin of the seamount-slope limestones is elucidated through petrography, geochronology and isotope geochemical analyses. Important questions to be addressed are: the relative roles of inorganic versus organic processes in the formation of the crusts, their rates of formation and the environmental factors involved, including water depth, temperature and fluid-flow related to hydrothermal systems.

2. Geological Settings

2.1 The Soufrière Hills Volcano, Montserrat

Montserrat is a predominantly andesitic volcanic island in the eastern Caribbean that is elevated to a height of almost 2 km above the surrounding seafloor from water depths of 800 to 1000 m. The island comprises four volcanic centres (Fig. 1) which become younger from north to south (Rea, 1974; Harford et al., 2002; Coussens et al., 2017; Hatter et al., 2018). These centres are the Silver Hills (2.17 to 1.03 Ma), Centre Hills (1.14 to 0.38 Ma), South Soufrière Hills (0.14 to 0.09 Ma) and the Soufrière Hills Volcano (SHV, 0.45 Ma to present). The major eruption of the SHV between 1995-2010 (Kokelaar, 2002; Wadge et al., 2014) has resulted in Montserrat being one of the most intensively studied island-arc volcanoes in the World. A striking feature of the island morphology is the development of a moderate-depth carbonate shelf (~ 120 to 140 m water depth) that becomes wider to the north / northeast of the island (figure 4 in Le Friant et al., 2004).

There are important tectonic structures in and around Montserrat. The island has developed at a major offset in a regional transtensional fault zone (Feuillet et al., 2010). To the SE of Montserrat, the Bouillante-Montserrat Fault Zone (Fig. 1) bounds a major half-graben to the east (Watt et al., 2012). The Havers-Montserrat fault system lies to the NW of Montserrat. The same fault zone, known as the Belham Valley fault, extends across the island between the SHV and Centre Hills along a WNW-ESE trend. The Belham Valley fault is a complex zone of deformation with localised uplift of the St George's and Garibaldi Hills. Lava domes, fumaroles and hot springs of the SHV are elongated along the fault zone (Wadge et al., 2014). A major geothermal field is centred on Belham Valley and St George's Hill to the NW of the SHV (Ryan et al., 2013). Seismic sections across the submarine fault-zone (Kenedi et al., 2010) show it is a major listric system downthrown to the NNE with multiple minor faulting across the footwall side with localised uplift in the hanging wall.

2.2 Kick'em Jenny volcanic field, Grenada

Kick'em Jenny submarine volcano (KeJ) is located just 7.5 km north of the island of Grenada in the southern Lesser Antilles (KeJ, Fig. 2). The first detailed bathymetric survey of the volcano in 1972 revealed a 1300 m high conical structure, constructed on the western flank of the arc with a summit crater at 190 m water-depth (Sigurdsson and Shepherd, 1974). Recent SEABEAM mapping of the volcano has shown that the summit cone and crater actually lie within a much larger arcuate collapse structure that opens to the west (Sigurdsson et al., 2006). A debris avalanche deposit associated with formation of the horseshoe-shaped collapse structure extends 17 km downslope into the back-arc Grenada Basin (Lindsay et al., 2005; Dondin et al., 2012) with chemosynthetic cold seeps at the distal end (Carey et al., 2014a). KeJ has erupted at least 12 times since 1939 and is currently the most active volcano in the West Indies (Devas, 1974; Lindsay et al., 2005). Some of the eruptions produce surface disturbances, subaerial plumes and minor tsunamis, whereas others have been detected only by T-phase seismic signals (Shepherd and Robson, 1967; Lindsay et al., 2005). Recent multibeam mapping and remotely-operated vehicle explorations of the area have revealed the presence of several other small volcanic centres just to the east and southeast of KeJ (Carey et al., 2015). The slopes of these centres, lying at about 200 metres water depth and apparently not recently active, exhibit common outcrops of carbonate crusts similar to those seen off the coast of Montserrat.

2.3 Kolumbo seamounts chain, Mediterranean

The seafloor northeast of Santorini volcano in Greece consists of a small, elongate rifted basin that has been the site of recent submarine volcanism (Kolumbo, Fig. 2). This area lies within the Cyclades back-arc region of the present-day Hellenic subduction zone where the seafloor of the eastern Mediterranean Sea is descending beneath the Aegean microplate. The Cycladic region and the Aegean Sea as a whole are known to be regions of south-easterly back-arc extension and thinning of continental crust. Nineteen submarine volcanic cones occur within this small rift zone, the largest of these being Kolumbo which last erupted explosively in 1650 AD, causing significant damage and fatalities on the nearby island of Santorini (Carey et al., 2011; Nomikou et al., 2012). Water depths of the submarine cones range from 18 to 450 metres. In general, the domes and craters northeast of Kolumbo are sediment covered and show little evidence of recent volcanic activity. Outcrops of volcanic rock can be found in the crater walls and slopes of some of the cones, but they typically

consist of volcanic fragments of pumice and lava, along with some bioclastic material, cemented by calcite, indicative of the lack of recent eruptions.

3. Methods and Samples

Multibeam mapping and remotely-operated vehicle (ROV) explorations of the submarine flanks of Montserrat, Kick'em Jenny and the Kolumbo seamount chain in the Mediterranean enabled submarine hardground occurrences to be imaged and sampled (Carey et al., 2011; Carey et al., 2014a,b; Watt et al., 2015; Carey et al., 2015). In addition to *in-situ* samples in the submarine environment, limestones have been sampled from three other settings on and around Montserrat. The first is from outcrops of submarine volcaniclastic sediment with thin (1-2 m thick) limestones on land at Roche's Bluff on the southeastern flank of Montserrat; a volcanic clast here has an $^{40}Ar/^{39}Ar$ age of 1.02 Ma (Harford et al., 2002). Second, geothermal boreholes in Belham Valley have recovered limestones interbedded with volcanics and intrusives in continuous core and in cuttings to depths of 2.3 km. And finally, Holocene offshore debris-avalanche deposits contain clasts of shallow-water coralgal limestone that have been transported into deeper water. Locations, water depths and brief descriptions of the samples are given in Table 1.

All limestone samples, including those from the geothermal borehole and Roche's Bluff outcrops, have been examined in thin-section, and some with SEM (scanning electron microscope). For stable isotope analysis of bulk carbonate the sample material was ground in agate and 10 mg of carbonate powder was reacted with anhydrous phosphoric acid in vacuo for 72 hours at a constant 25°C (Ca and Mg carbonates including dolomite should react within this time) at the British Geological Survey (BGS). The CO_2 liberated was separated from water vapour under vacuum and collected for analysis. Measurements were made on a VG Optima mass spectrometer at BGS Keyworth, UK. Overall analytical reproducibility for these samples is normally better than 0.2‰ for $\delta^{13}C$ and $\delta^{18}O$ (2σ). Isotope values ($\delta^{13}C$, $\delta^{18}O$) are reported as per mil (‰) deviations of the isotopic ratios ($^{13}C/^{12}C$, $^{18}O/^{16}O$) calculated to the VPDB scale using a within-run laboratory standard calibrated against NBS standards (Table 2).

Samples selected for strontium isotope ($^{87}Sr/^{86}Sr$) seawater-age determinations were measured in the Bristol Isotope Group facility at the University of Bristol. Following the protocol described in Lewis et al. (2014), samples were dissolved in high purity acids and Sr separated using Sr Spec resin (Horwitz et al., 1992). Samples were loaded on to single

rhenium filaments with a $TaCl_5$ activator (Birck, 1986) and Sr isotope ratios were measured using a Thermo-Finnigan Triton thermal ionization mass spectrometer. Samples were measured using a multi-dynamic 'triple-jump' method (Thirlwall, 1991; Avanzinelli et al., 2004) of 200 cycles with a 4.194 s integration time per cycle. Instrumental mass bias was corrected using an exponential mass bias law and an $^{86}Sr/^{88}Sr$ of 0.1194 (Nier, 1938; Russell et al., 1978); ^{87}Rb is corrected by monitoring ^{85}Rb and using an $^{85}Rb/^{87}Rb$ of 2.59265 (Steiger and Jäger, 1977). Long-term reproducibility of $^{87}Sr/^{86}Sr$ for NIST SRM 987 processed through column chemistry is 0.710247 ± 0.00001 (2 SD, n = 58). Results are given in Table 3.

4. Petrography of carbonate crusts: facies, diagenesis and interpretations

4.1 Montserrat submarine slope limestones

Multibeam images of the western and south-western flanks of the SHV are shown in Fig. 3. A limestone crust occurs as a continuous layer covering many square km of the submarine slope surface from water depths of several hundred to nearly 1000 metres, as observed and videoed by the ROV. The crust shows abrupt boundaries where large slabs have broken off and detached, indicating mass wasting. Figures 4a and 5a show images of limestone slabs where they have been locally disrupted and tilted, revealing their internal texture and lithology. The surface crusts vary from several 10s of cm to several metres in thickness and below, less-well lithified and unlithified sediment is exposed. The limestone crusts are typically made of volcaniclastic material (boulder to silt grade), containing variable amounts of bioclastic debris, all cemented by carbonate. There are also crusts largely composed of carbonate skeletal debris with subsidiary volcanic clasts. These are strongly lithified rocks and contrast with the unconsolidated and uncemented volcaniclastic deposits that form when lahars and pyroclastic flows enter the ocean from the island (Le Friant et al., 2009; Trofimovs et al., 2012).

Samples of cemented slope limestone were collected by ROV from the nearshore area to the SW of Montserrat. Two samples were located some 1-2 km from the shoreline (Fig. 3), at 188 m water depth (NA037-029) and 292 m (NA037-033). Both came from seafloor exposures of limestone crust where pieces had broken off (Figs. 4 and 5). Two other limestone samples were located about 8 km from the shoreline (Figs. 6 and 7) and are associated with the debris avalanche known as deposit 5 (Le Friant et al., 2004), formed between 8 and 12 kyr (Cassidy et al., 2013) due to collapse of the shallow shelf platform.

Sample NA037-025 comes from 806 m water depth, again where an extensive cemented seafloor is present and NA037-026 from 823 m.

Sample NA037-029 is a bioclastic volcanic-grain pack-grainstone with some pebble-sized volcanic clasts (Fig. 4a, b). Some granules-pebbles are coated by calcareous red algae (giving rhodoliths)(Fig. 4b); the sandy (< 2 mm) sediment consists of fragments of red and green calcareous algae (including *Halimeda*), foraminifera (several *Amphistegina*), bivalve, serpulid and echinoid. The sediment is moderately-well sorted with some larger coated grains. There are sponge borings in shells (Fig. 4c), filled with sediment, but these borings also penetrate the sediment, indicating an earlier phase of cementation. The micritic sediment contains diffuse peloids, and possible filaments, probably of microbial origin. In areas of intergranular pores and cavities, a fibrous-bladed isopachous calcite fringe occurs around grains (Fig. 4d). This rock was likely deposited from a sediment gravity flow or landslide and has been cemented *in situ* by a micritic and fibrous calcite cement to form a hardground.

Sample NA037-033 is also a true hardground from synsedimentary cementation of the submarine slope (Fig. 5a). It is a bioclastic volcaniclastic grainstone (Figure 5b), with larger clasts up to several cm, consisting of numerous shallow-water bioclasts: foraminifera (*Amphistegina*, *Peneroplis*, miliolinids), bivalves, gastropods, echinoids, calcareous algae – both red and green (*Halimeda*), and volcanic grains coated with calcareous red algae, serpulids and encrusting foraminifera (Figs. 5b-d). Planktic gastropods (pteropods and heteropods) are present as well as planktic foraminifera. Peloids, probably microbial, occur within cavities in a geopetal arrangement (Fig. 5d). The main cement between grains consists of either an isopachous bladed calcite fringe or an isopachous micritic fringe (Figs. 5e, f). Within gastropods there are acicular aragonite cements, syntaxial upon the shell. There is still much empty pore space. This deposit is interpreted as resedimented, consisting of a mixture of volcanic crystals and clasts and shallow-water skeletal debris. However, there is also a planktic component indicating some mixing with pelagic sediment during slope transport.

Sample NA037-025 is a loose piece of cemented sand (Fig. 6a) from a deep-water slope within an area of surface crust. The sediment is extremely well sorted with all grains being medium to coarse sand-size. There is a high content (90%) of bioclasts: shallow-water foraminifera (peneroplids), calcareous algae (branched forms), green algae (*Halimeda*, aragonitic, some with evidence of dissolution) and bivalve fragments (Fig. 6b). Volcanic grains are a minor content (10%). Peloids are present in cavities between grains and are probably microbial in origin. The cement is a bladed isopachous calcite, with polygonal

junctions between fringes, typical of marine phreatic precipitation (Figs. 6c, d). Acicular aragonite cement occurs within gastropod shells, a syntaxial effect (Fig. 6d).

Sample NA037-026 is a loose sample from an area of rocky outcrops on a quite steep slope (Fig. 7a). It consists of relatively well-sorted granule-small pebble sized volcanic clasts and crystals, many coated with crusts of calcareous red algae (*Amphiroa*, *Lithoporella*), foraminifera (including nubeculariids and acervulinids), serpulids, bryozoans and microbial laminae (Figs. 7b-d). Calcimicrobe filaments are present (like *Girvanella*), with some being beaded (like *Rothpletzella*, Rob Riding pers. comm.). Pockets of phosphatic peloids are likely also microbial-bacterial. Other bioclasts present include benthic foraminifera (*Amphistegina* and *Archaias*) and echinoids. Evidence of dissolution is present in the form of bivalve and heteropod-gastropod molds (Fig. 7e), some filled with calcite spar. Sponge spicules are also present and show dissolution and replacement by calcite. The patchy cement is mostly a sparry calcite with a drusy fabric. The benthic foraminifera are both from long-ranging genera spanning the Eocene to Holocene and Middle Eocene to Holocene (Boudagher-Fadel, 2008); the random orientation of sections prevents further identification to species level.

For both samples 025 and 026 the bioclastic and coated volcanic grain sediment must have formed in much shallower water but then been transported to these deeper locations by either a sediment gravity flow or submarine landslide, where the induration took place. Some deeper-water bioclasts are also present (the heteropods, planktic foraminifera and sponge spicules), probably picked up en-route.

In some cases, the cemented slope surfaces are coated with a thin layer of black Mn-Fe oxide-hydroxide, which also occurs on submarine outcrops of volcanic rock. This distinctive surface usually has a very irregular topography of 1-2 cm which likely reflects the effects of boring organisms and local dissolution. Such Fe-Mn oxide coatings are typical of deeper-water lithified surfaces and rock outcrops in areas of sediment starvation and/or where there are quite strong currents sweeping the seafloor. Phosphate (honey-brown colour in thin-section) may also be present, and commonly planktic foraminifera are trapped within the coating. The origin of these Mn-Fe surfaces has been much debated but a bacterial origin is suspected in many cases (Konhauser, 1998). Indeed, tufts of *Frutexites* bacteria have been observed in a thin-section of one such coating of a volcanic rock from a depth of 616 m, 25 km ESE of Montserrat.

4.2 Montserrat submarine debris-avalanche deposits

Submarine debris-avalanche deposits are a prominent feature of the seafloor around Montserrat (Le Friant et al., 2004; Cassidy et al., 2013; Watt et al., 2015). Off the east coast the youngest debris avalanche, deposit 1, is attributed to the formation of English's Crater by sector collapse at about 4 kyr BP. Three samples of limestone were collected from deposit 1 (Fig. 2).

Sample NA037-005 (depth 942 m and 12 km offshore) consists of a grey-green micritic pelagic limestone with numerous planktic foraminifera (*Globorotalia*, *Orbicula*), pteropods, thin-shelled planktic gastropods (heteropods), minor fragments of shallow-water bioclasts (bivalve, foraminifera, echinoid), and silt-sized volcanic crystals. There are some mm-size burrow structures.

Samples NA037-002 (975 m depth and 12 km offshore) and **NA037-012** (840 m depth and 6 km offshore) are of a similar shallow-water microfacies. Sample NA037-002 is a highly indurated carbonate with coralline algal fragments and small volcanic lithics. Large (cm-size) rhodoliths (nodules of calcareous red algae) occur in a matrix of micrite with many bioclasts, including bivalves, gastropods and benthic foraminifera (*Amphistegina, Archaias* and peneroplids). Patches of drusy calcite spar occur in cavities and occupy moulds of bivalves. Sponge borings occur in the rhodoliths, some filled with microbial peloids. Sample NA037-012 is also coralgal limestone with rhodoliths and a variety of bioclasts including peneroplid foraminifera and bivalves, some showing effects of dissolution and replacement of aragonite by calcite. Encrusting forams and peyssonneliacean algae are present. Volcanic material is subordinate. Samples 002 and 012 are both shallow-to-moderate (<50 m) depth limestones with typical lagoonal forams. The diagenetic features are consistent with meteoric / freshwater alteration (Tucker and Wright, 1990), although meteoric-type cements can form in deeper water (Schlager and James, 1978; Melim et al., 1995, 2002).

Overall, these samples represent limestones from the shallow shelf dislodged and incorporated into the debris avalanche. Sample 002 contains a single probable miogypsinid fragment, which would give a Miocene age; the fragmentary nature of the bioclast however means that reworking is a possibility, although this does agree with the Sr data. However, other genera present again have long ranges from Eocene to Holocene.

4.3 Roche's Bluff submarine volcaniclastic unit, Montserrat

Limestones within a package of submarine volcaniclastics exposed at Roche's Bluff in the SE corner of Montserrat are much fractured and deformed, but fabrics are quite well preserved in thin-section, with some patchy recrystallisation. MacGregor (1938) identified

corals, echinoid spines, serpulids, bivalves and ostracods in the limestones. In our samples the rock is a coralgal limestone with fragments of volcanic rock, many coated with coralline algae and encrusting foraminifera (including nubeculariids). Gastropods and bivalves are present (aragonite shells replaced by calcite), and benthic foraminifera: miliolids, *Amphistegina*, poorly preserved *Archaias*-type forms, miogypsinids, rare planktic foraminifera and agglutinating textularid foraminifera. There are two generations of calcite cement: fibrous fringes and drusy spar, and minor aragonite cement has been replaced by calcite. This limestone was deposited in a shallow-moderate depth, relatively high-energy location and then subsequently uplifted to its present location. It was subjected to marine cementation and also meteoric dissolution-cementation. The presence of multiple sub-axial sections of *Miogypsina* indicates an early Miocene age in the Americas (BouDagher-Fadel, 2008); the specimens do appear to be complete.

4.4 Montserrat geothermal wells

Exploration for geothermal energy on Montserrat included three drill-sites. Continuous core was collected in Well-3 at depths of 1.5, 1.7 and 2.0 km and rock cuttings were recovered at all levels. Of most relevance here are two horizons of limestone at 2014-2016 m and 930-1020 m depth, within a succession dominated by volcanic, volcaniclastic and intrusive rocks. The limestones at 2014-2016 m, showing evidence of recrystallisation, are mostly fossiliferous wackestone to pack-grainstone from shallow to moderate depths, normal open-marine water. From the foraminifera, a late Miocene age has been assigned (Marcelle BouDagher-Fadel, personal communication). Limestones from depths 1020 to 950 m are also highly fossiliferous and indicate an upward trend from shallower to deeper water. Sample 930 m contains abundant planktic foraminifera, including likely *Orbulina universa,* a single potential *Globergerinoides sacculifer* and potential *Globorotalia* with *Trilobatus trilobus* indicating a likely age in the last 5 Ma.

4.5 Kick'em Jenny, Southern Lesser Antilles

Two samples are highlighted from the area of Kick'em Jenny submarine volcano in the southern Lesser Antilles (Fig. 2).

NA039-071 is a partially indurated carbonate found in proximity to a cold-seep area associated with the distal end of a large debris avalanche on the western slope of KeJ at a depth of 1956 m (Figs. 2, 8a). The seeps host a chemosynthetic-based ecosystem with

bivalves, tubeworms, gastropods, crabs and holothurians (Carey et al., 2014a, b, c). The hand-sample contains large burrows, up to 20 mm in diameter, some of which are open whereas others contain intraclasts and pellets, up to 7 mm in diameter (Fig. 8b, c). In thin-section the sediment consists of grey-green pelagic lime mud and silt with many tiny microfossils including planktic forams (100-500 microns across) and fine skeletal fragments (<200 microns). However, conspicuous are relatively large ostracods, up to 3 mm across (Figs. 8c, d). Some of these ostracods with a mud-fill appear to be part of the large pellets within burrows. Isopachous fibrous-bladed calcite cement occurs locally around the pellets (Fig. 8d). Within one ostracod an acicular cement is present, appearing more like aragonite. Of note, as reported later, this sample has an extremely low $\delta^{13}C$ of -42‰.

NA039-035 is from the upper slopes of the Kick'em Jack submarine volcano at 172 m depth (Fig. 2) and consists of a mixture of volcanic grains, bioclastic material and lime mud (Fig. 9a). Mafic crystals commonly have a reaction rim. The matrix consists of silt-grade volcanic particles and lime mud which appears to have infiltrated cavities between grains. This mud is vaguely peloidal, but locally it grades into a clear micropeloidal texture. There are pockets of micropeloids, with no matrix between, occurring within cavities which are lined by an initial, very thin isopachous honey-brown amorphous material (Fig. 9b). These micropeloids, 10-30 µm in diameter, appear to have formed within the cavities rather than being washed in, suggesting an in-situ microbial origin. There are also larger peloidal structures (30-60 µm), some coalesced, composed of phosphate. In the patches of lime mud, there are planktic forams, fine bioclastic debris and sponge spicules, replaced by calcite; spicules also occur within empty cavities, which may well have been sponge borings.

4.6 Kolumbo seamount chain, Mediterranean

The numerous seamounts extending northeast from the Santorini caldera show little evidence of recent volcanic activity, with the exception of Kolumbo, which is mostly sediment covered with local outcrops of volcanic rock (Nomikou et al., 2012). Many of the slopes of the seamounts consist of brown, carbonate crusts that are commonly fractured into slab-like pieces. The crusts are typically tens of centimetres to a few metres in thickness with a thin draping of unconsolidated hemipelagic sediment. The sampling locations of three representative samples of carbonate crust from this area are shown in Fig. 2. Samples NA007-001 and NA007-045 are from a small dome complex on the northeast margin of the Kolumbo submarine volcano in water depths of 200 and 128 metres respectively (Fig. 2).

Sample NA007-022 was collected from a depth of 194 m on a separate small seamount about 7 km northeast of Kolumbo.

Sample NA007-001 is a pelagic limestone with many microfossils, planktic forams, thin-shelled bivalves as well as fragments of sponge spicules. The sample itself shows the effects of boring sponges (Fig. 10a). Indeed, an earlier phase of boring has cavities filled with a more brownish lime mud compared to the host lime mudstone that has more of a grey colour. Later sponge borings are open and there are modern encrusting serpulids and other organisms present too.

Sample NA007-022 (Fig. 10b) has granule to pebble-sized volcanic clasts coated by calcareous red algae, with lime mud containing microfossils between. The sample has also been bored by sponges and cavities are in places lined by a bladed calcite fringe before a later phase of more microfossiliferous lime mud filling cavities (Figs. 10c, d).

Sample NA007-045 is from slightly deeper water (128 m), on the side of a very small volcanic dome (Figs. 2, 11a). This is a crustose limestone composed of an open framework of foliaceous coralline algae, encrusted with bryozoans and serpulids, with fine-medium sand and volcanic-bioclastic material occurring within the framework cavities (Figs. 11b-d). Fibrous calcite cements occur here as crusts and fans.

These samples from the Hellenic Arc in the Mediterranean are similar to the crusts from the Caribbean: a variable mixture of volcanic and bioclastic material, the biota depending on water depth and degree of downslope reworking of skeletal grains; early cementation commonly by fibrous calcite and micritic calcite; several phases of sponge boring with lime mud, usually pelagic, filling cavities and latest borings still empty, and crusts in deeper water showing thin Fe-Mn coatings.

5. Isotope data and interpretations

A cross-plot of the $\delta^{13}C$ and $\delta^{18}O$ data from Montserrat limestone samples is given in Fig. 12 and the data are presented in Table 2; the results of $^{87}Sr/^{86}Sr$ analyses and approximate ages derived therefrom are given in Table 3. The apparent ages of carbonate samples can be estimated based on strontium isotopic ratios in comparison with the global seawater strontium isotope curve and data from Neogene carbonates (e.g. Farrell et al., 1995; Howarth and McArthur, 1997 – LOWESS Database 2013; McArthur et al., 2006; McArthur et al., 2012). This approach assumes that the carbonate minerals have been precipitated from seawater and that they have not subsequently been perturbed. However, some of the limestones, notably those from the geothermal well, have ages that are apparently much older

than those indicated by foraminifera, suggesting that their initial Sr isotopic compositions have been altered. This is interpreted to have been through contact with geothermal fluids and, in this respect, the $\delta^{13}C$ and $\delta^{18}O$ isotope data can be used to confirm that alteration has taken place, as discussed in more detail below.

5.1 Montserrat submarine slope limestones

Samples of slope crusts NA037-033 and NA037-029 from nearshore SW Montserrat have young Sr isotope ages of less than 200 kyr and very similar $\delta^{13}C$ and $\delta^{18}O$ values, averaging +3.6 ‰ and +2.25 ‰ respectively (Tables 2, 3 and Fig. 12). The $\delta^{13}C$ are within the usual range of marine sediments (Tucker and Wright, 1990), whereas the $\delta^{18}O$ is a little more positive than might be expected for a tropical carbonate (e.g. Swart, 2015). This could be the consequence of cementation in water > hundred metres deep, which would have been quite cool (~13-20 ºC), compared with a near-surface water temperature of 28-30 ºC (Kameo et al., 2004). Sample NA037-025 from offshore SW Montserrat also has a young Sr isotope age (a few 100 kyr) and similar marine values for both $\delta^{13}C$ (+3.2‰) and $\delta^{18}O$ (+2.5‰). In contrast, sample NA037-026 has a much older apparent Sr isotope age (17-20 Ma) and low negative stable isotope values for both $\delta^{13}C$ of -2.3‰ and $\delta^{18}O$ -3.8‰, suggesting alteration.

5.2 Montserrat submarine debris-avalanche deposits

The three limestone clasts collected from within Montserrat debris-avalanche Deposit 1 on the eastern side of the island have diverse isotope geochemistry. The pelagic limestone (sample NA037-005) has a very young Sr isotope age (<100 kyr) and typical marine values for $\delta^{13}C$ and $\delta^{18}O$. The two coralgal limestone clasts (NA037-002 and NA037-012) have yielded much older Sr age dates, especially sample NA037-002, of 23-25 Ma (early Miocene), whereas sample NA037-012 is 975 kyr to 1.5 Ma (Table 3). For the C and O isotopes, sample NA037-012 has low positive values (Fig. 12), both likely marine. Sample NA037-002, on the other hand, has a typical marine $\delta^{13}C$ signature (+2‰) but $\delta^{18}O$ varies, with 4 negative values (-2.5 to -3.6‰) and one of +2‰. The negative $\delta^{18}O$ values are consistent with some alteration, likely meteoric, reflecting the low negative isotopic composition of freshwater (mean rainfall is ~-4‰ $\delta^{18}O$ VSMOW for Barbados for example). The $\delta^{13}C$ values indicate recycling of the original marine carbonate, rather than any effect of soil CO_2 gas which would be enriched in (biogenic) ^{12}C (Tucker and Wright, 1990).

5.3 Roche's Bluff submarine volcaniclastic unit, Montserrat

Roche's Bluff limestone samples also yield apparent old Sr isotope ages: 16.5 and 17.1 Ma (early Miocene), which are inconsistent with other age data, such as the $^{40}Ar/^{39}Ar$ age of 1.021 ±0.020 Ma from a volcanic clast in the Roche's Bluff submarine volcaniclastic unit and the <1.8 Ma age suggested by the identification of the foraminifera species *Globorotalia truncatulinoides* (Harford et al., 2002). However, the presence of several *Miogypsina* in the thin-sections would support a Miocene age, although other larger foraminifera present only indicate Eocene to Recent. The $\delta^{13}C$ values are normal marine (average +2.1‰). However, $\delta^{18}O$ values are very negative at -7.7‰; this is too low for rainfall of this latitude for it to be simply a meteoric / freshwater effect. An alternative explanation is that the low negative $\delta^{18}O$ of the Roche's Bluff limestone was generated by recrystallisation (recorded in thin-section) under moderate-high temperatures through interaction with hydrothermal fluids. This would also account for the apparent old Sr ages, if the miogypsinids are reworked. Such hydrothermal fluids, with a low Sr isotope value derived from passage through volcanics, may have been introduced through the fault system adjacent to the Roche's Bluff outcrops.

5.4 Montserrat geothermal Well-3

For limestones in the geothermal Well-3 the apparent Sr isotope ages are all much older than the ages based on fossils and unpublished $^{40}Ar/^{39}Ar$ data. The core samples of upper Miocene (~5-7 Ma) limestone at 2 km depth, confirmed by foraminifera (Marcelle BouDagher-Fadel, personal communication), give much older apparent Sr ages in the range 16.7-19.7 Ma. Cuttings samples from 930 m and from 1198 m depth are also apparently old: 4 analyses give an age of around 15 Ma, although one analysis yielded an age of 0.55 Ma; the planktic foraminifera do suggest a young age. Unpublished $^{40}Ar/^{39}Ar$ ages of andesites at depths of 1.5 and 1.7 km depth are approximately 1 Ma old. The C and O isotope data from two (whole-rock) limestone core samples both have negative $\delta^{13}C$ and $\delta^{18}O$. For one sample (2015 m depth) $\delta^{13}C$ values (4 analyses) are low (average -0.75‰), with very negative $\delta^{18}O$ values (average -10.3‰). For sample depth 2016 m, $\delta^{13}C$ values (2 analyses) are more negative (average –3.2‰) and $\delta^{18}O$ averages -9.4‰. One analysis from a thick-shelled bivalve in that 2016 m sample has values of +1.9‰ for $\delta^{13}C$ and -11.2‰ for $\delta^{18}O$. The negative $\delta^{13}C$ values are likely the result of decomposition of organic carbon within the sediments, producing isotopically light CO_2. For cuttings samples (930 m to 1198 m), $\delta^{13}C$ and $\delta^{18}O$ values are around +2‰ for $\delta^{13}C$, a typical marine carbonate value, but $\delta^{18}O$ is -8‰, again suggesting significant alteration related to burial diagenesis / interactions with

hydrothermal fluids, although these had no effect on the $\delta^{13}C$, possibly related to issues around supply or availability of C in the fluid.

These Sr and stable isotope analyses from the Mon3 well all indicate post-depositional alteration of the original seawater-marine values, most likely by interaction with hydrothermal-volcanic fluids. The apparent old ages are the result of introducing a component of volcanic non-radiogenic Sr into the carbonates. $^{87}Sr/^{86}Sr$ values of Montserrat volcanic rocks are in the narrow range 0.7035 to 0.7038 (Cassidy et al., 2012). The Sr in the geothermal fluids will be largely derived from the volcanic rocks and this will exchange with or add to the limestones' initial Sr. Likewise, the strongly negative $\delta^{18}O$ reflects geothermal fluid interactions.

Thus, we surmise that the anomalously old Sr ages and negative $\delta^{18}O$ in samples from the Deposit 5 debris avalanche (NA037-026), the Deposit 1 debris avalanche (NA037-002) and the Roche's Bluff limestone, are also the consequence of hydrothermal alteration of shelf and slope limestones.

6 Discussion and conceptual model

6.1 Montserrat seamount slope hardgrounds

All the features of the Montserrat seafloor hardgrounds are consistent with the volcaniclastic-carbonate sediment being cemented and altered on the seafloor in the marine environment. They are similar to crusts reported by Thompson et al. (1968), Schroeder et al. (2002), McKenzie and Bernoulli (1982) and Buchs et al. (2018). The bioclastic material in the slope limestones described here is dominated by calcareous red algae, especially in the form of rhodoliths, encrusting volcanic grains, and foraminifera, both benthic (including encrusting) and planktic, the former commonly derived from shallower water. Rhodoliths are a common feature of limestones associated with volcaniclastic and volcanic rocks, especially in the moderate to high-energy settings of open-ocean seamounts and islands (e.g. Madeira and the Azores: Baarli et al., 2014; Rebelo et al., 2016), and they are readily transported into deeper water.

Micritic peloids are a feature of many Montserrat crusts, occurring within intraskeletal cavities, borings and between grains, and in some cases there is a gradation into micritic sediment. Microbial filaments are also present but they can be difficult to distinguish from nubeculariid foraminifera or thin poorly-preserved coralline algal crusts. Petrographic evidence for microbial activity is being recognized more frequently as the significance of

microbes in mineral precipitation is becoming appreciated (e.g., Perri et al., 2018). Here in these crusts, communities of bacteria living within the sediment are implicated by the occurrence of the peloidal micrite and it may well be that microbial processes contributed to the lithification of the slope sediment. Some bacteria promote carbonate precipitation, notably the cyanobacteria and sulphate reducers, by raising alkalinity, leading to the formation of micritic cement, whereas others, such as aerobic heterotrophs and fermenters, may lead to local carbonate dissolution through reducing pH in their metabolic processes (Dupraz et al., 2009). Dissolution of the surface of the hardgrounds is evident from their irregular microtopography, and some of this may be microbial, and a mm-thick layer of Mn-Fe oxide coating is a common feature, also likely microbial.

Reviewing the diagenesis observed within the crusts, the most common cement is calcite, in many cases a bladed-fibrous type, particularly as an isopachous rim around grains in the more porous well-sorted, sand-grade deposits. Other crusts have a drusy sparry calcite cement within cavities. Acicular aragonite crystals mostly occur as syntaxial precipitates on originally aragonitic skeletal fragments, especially gastropods, but these may be shallower water bioclasts reworked downslope into deeper water. Evidence of aragonite dissolution and replacement is provided by molds of bivalves, some filled with calcite. Sponge spicules (originally opaline silica) have also been replaced by calcite, with crystals extending out into cavities. Several phases of boring by sponges are evident as well as phases of internal sedimentation.

Calcite spar as a cement is usually regarded as a near-surface meteoric or burial precipitate, but there are records of it occurring on the seafloor in deeper water (Melim et al., 1995, 2002). Slower rates of precipitation in cooler water are the likely explanation. Cooler water and its circulation through the surficial crusts are likely to account for aragonite dissolution and replacement, again a feature commonly ascribed to freshwater diagenesis (Tucker and Wright, 1990), but here occurring in moderate depth seawater. All in all, the paragenesis of these crusts is commonly a complex series of cementation-alteration-boring-dissolution events.

The formation of hardgrounds in the deeper-water slope environment from influxing seawater is controlled by several factors, but notably carbonate saturation, the movement of fluid through sediment (the 'hydrodynamic level' of Christ et al., 2015) and the microbial activities, as well as temperature and a sediment's poroperm. At the depths of less than 1000 m where the cemented crusts occur seawater will be saturated with respect to $CaCO_3$, even though seafloor temperatures will be down to 5ºC (Kameo et al., 2004). The circulation of

fluid through sediment is essential to drive cement precipitation and here waves and tides, internal waves and ocean currents impinging on a slope may all be involved (van der Kooij et al., 2010). In addition, circulation driven by geothermal heat within the seamount (see later Section 6.4), is likely to contribute to drawing in water from the adjacent sea (Jones et al., 2000).

6.2 Limestones showing evidence of hydrothermal alteration

Most of the limestones in the geothermal wells, two clasts of shallow-water limestone taken from debris-avalanche deposits, and the Roche's Bluff limestone, all show isotopic evidence for hydrothermal alteration with very negative $\delta^{18}O$ values and $^{87}Sr/^{86}Sr$ compositions that indicate ages from the seawater calibration curve that appear to be too old compared to ages derived from foraminifera. We infer that these limestones have been affected by the volcanogenic hydrothermal systems that developed within the island interior. The observed alteration testifies to largescale hydrothermal convection throughout the island's history.

6.3 Slope hardgrounds and seamount stabilisation

The formation of seamount hardgrounds is inferred to be in the mature stage of volcanic edifice growth. Each of the volcanic centres in the Montserrat area initially formed on the seafloor at water depths of 800 to 1000 m and grew to a height of the order of 1000 m above sea level, as is the case for the still active Soufrière Hills Volcano. For a constant rate of volcanism the lateral speed of advance of the volcanoes' flanks will slow; for example if the edifice is treated as a cone with a constant height to width ratio then the lateral speed will decrease in proportion to $t^{-2/3}$.

There is geomorphological evidence for the stabilisation of the submarine flanks of Montserrat and their preservation for long periods of time. Le Friant et al. (2004) compared several topographic profiles around Montserrat from the shallow shelves to deep water. The overall width of the shallow part of the island stays approximately the same from north to south (Fig. 1) whereas the shallow shelf decreases in width. The profiles from the shelf edge to deep water are very similar. These observations suggest that the submarine parts of the island stabilized after the volcano became extinct, which can be explained by the formation of the limestone crust which prevented inward erosion by mass wasting. The widening of the shallow shelf from south to north was interpreted by Le Friant et al. (2004) as the consequence of lateral erosion of the island during glacial highstands due to wave and storm

erosion. However, there is new evidence for regional subsidence (Carey et al., 2019) and so the widening of the platform to the north could also reflect subsidence of the three volcanic centres on Montserrat, which become older to the north. In either case the platform outer edge will approximately reflect the width of the final edifice at the cessation of volcanic activity.

On the western side of Montserrat, there is further evidence for stabilisation of the submarine flanks from the marked embayments and southward narrowing of the shelf. This zone is the location of where active faults of the Havers-Montserrat fault system intersect the island. We suggest that faulting in this zone has disrupted the limestone crust and promoted mass-wasting of the submarine flanks. Furthermore, episodes of sector collapse can play an important role in that they would channelize lahars and pyroclastic flows down preferential pathways, as exemplified by the Tar River Valley on the eastern flanks of Montserrat. As a consequence, large sections of submarine coast will be abandoned with lateral growth reducing or ceasing, providing conditions for thick limestone crust to form. The subsequent disruption and collapse of the surficial cemented seafloor sediment will then form an archive of the frequency distribution of slope failure.

6.4 Model for seamount seafloor slope carbonate cementation

We propose a conceptual model for the development of limestone hardgrounds on the slopes of seamounts based on established groundwater models for coastal regions and volcanic islands (Cooper, 1959; Join et al., 2005), perturbed by the development of a hydrothermal system (Fig. 13). Montserrat broadly conforms to the conceptual model (Hemmings et al., 2015) of a freshwater lens above sea level and saline (seawater) intrusion beneath with a transitional mixing-zone occurring close to the coast. Freshwater outflows at the coast are balanced by recharge and seawater inflow below sea level. The hydrogeology on Montserrat is significantly perturbed through the development of a geothermal field along the Belham Valley fault system (Ryan et al., 2013) and the presence of an active hydrothermal system associated with the SHV edifice. Several scattered fumaroles and hot springs have been present historically (Chiodini et al., 1996), although these systems were disrupted by the 1995-2010 eruption. The Belham Valley geothermal field contains brines with the approximate salinity of seawater, but with a geochemistry suggestive of interaction with volcanic rocks. Temperatures up to 230 ^{o}C are recorded in the geothermal wells.

We envisage that the seafloor carbonate crusts largely developed as a result of carbonate-saturated seawater fluxing through the submarine flanks of the island, precipitating

carbonate cement in the pores of the sediments. The $\delta^{13}C$ and $\delta^{18}O$ values of many of the crust samples indicate a seawater origin. In the classic coastal hydrological model (Fig. 13) the main driver is the density difference between seawater and fresh groundwater in the volcanic edifice. The subaerial flanks of the volcano are composed of high permeability and high porosity volcaniclastic deposits which create the main aquifer (Hemmings et al., 2015).

Two factors can enhance the submarine inflow of seawater into the volcanic edifice. Upwelling of hot geothermal and hydrothermal magmatic fluids within the volcanic island is expected to cause inward flow of groundwater and underlying brines, strengthening the inflow of seawater. The process of Kohout convection, driven by geothermal heat, has long been invoked as a mechanism for drawing seawater into carbonate shelves and isolated platforms, and precipitating dolomite (Whitaker and Smart, 1990). In addition, inflow will be enhanced by strong ocean currents impinging on the seamount, and these will be increased during periods of sea-level rise due to the increased hydraulic head in the ocean (Tucker, 1993; Kim et al., 2010). There have been changes in sea level on the scale of up to 100 m many times over the last few million years as a result of the waxing and waning of Quaternary ice sheets. The inflow, however, may decrease as the carbonate crust forms, with consequent reduction of porosity and permeability, so that the formation of the crust may then promote sealing of the island interior from seawater intrusion.

7. Conclusions

Remotely-operated vehicle (ROV) explorations of shallow to moderately deep seamounts in many subduction zone environments, such as the Lesser Antilles (West Indies) and Hellenic Arc (Greece), reveal the existence of extensive carbonate crusts on their submarine flanks. These crusts are composed of mixtures of volcaniclastic debris and bioclastic material, in most cases cemented by calcite, in the form of isopachous coatings around grains or pore-filling spar. $^{87/86}Sr$ isotope data give an indication of age but also demonstrate that some samples are altered by hydrothermal-volcanic processes, as shown by ages much older than expected. Such alteration is also supported by $\delta^{13}C$ and $\delta^{18}O$ isotope data, although most samples possess typical marine values, with the $\delta^{18}O$ commonly a little more positive, likely reflecting cooler water at the depth of carbonate lithification. The occurrence of such hardgrounds on the slopes of seamounts and volcanic islands is significant from two perspectives. First, they represent a poorly-documented occurrence of limestone deposition in the World's oceans. The hardgrounds generated also form important hard substrates for the

development of benthic biological communities. Second, the hardgrounds act to protect the submarine flanks of volcanic islands and seamounts from erosion and collapse and they may inhibit submarine intrusion of seawater into the interior of such volcanic edifices.

Acknowledgements

Leverhulme Trust Emeritus Fellowship to RSJS. We are grateful to Marcelle BouDagher-Fadel for the identification of foraminifera in the Montserrat Well-3 core samples, to Paul Pearson for advice on planktic foraminifera, to Juan Carlos Braga for comments on coralline algae and Rob Riding for thoughts on calcimicrobes. NERC are thanked for funds to allow coring of the Montserrat geothermal drill holes and the BGS for archiving of and access to the cores. Cruises of the E/V Nautilus were supported through grants from the Office of Ocean Exploration (NOAA). Nicole Raineault provided valuable assistance in the processing and preparation of multibeam maps of the slopes of Montserrat. We are grateful to reviewer Adrian Immenhauser and the journal editor Edward Anthony for their useful comments on the MS.

References

Aghib, F.S., Weissert, H., Bernoulli, D., 1991. Hardground formation in the Bannock Basin, Eastern Mediterranean. Mar. Geol. 100, 103–113.

Allouc, J., 1990. Quaternary crusts on slopes of the Mediterranean Sea: a tentative explanation for their genesis. Mar. Geol. 94, 205–238.

Avanzinelli R., Boari E., Conticelli S., Francalanci L., Guarnieri L., Perini G., Petrone, Chiara M., Tommasini S., Ulivi M., 2005. High Precision Sr, Nd and Pb Isotopic Analyses Using the New Generation Thermal Ionisation Mass Spectometer ThermoFinnigan Triton-Ti. Periodico Di Mineralogia 74, 147–66.

Baarli, B.G., Cachão, M., da Silva C.M., Johnson, M.E., Mayoral, E.J., Santos, A., 2014. A Middle Miocene carbonate embankment on an active volcanic slope: ilhéu de Baixo, Madeira Archipelago, Eastern Atlantic. Geol. J. 49, 90–106.

Birck, J.L., 1986. Precision K-Rb-Sr isotopic analysis: application to Rb-Sr chronology. Chem. Geol. 56, 73-83.

Boudagher-Fadel, M. K., 2008. Evolution and geological significance of larger benthic foraminifera. Amsterdam: Elsevier, Developments in Palaeontology and Stratigraphy, 21, 544 p.

Buchs, D.M., Williams, R., Sano, S.I., Wright, V.P., 2018. Non-Hawaiian lithostratigraphy of Louisville seamounts and the formation of high-latitude oceanic islands and guyots. Journal of Volcanology and Geothermal Research 356, 1-23.

Carey, S., Bell, K.L.C., Nomikou, P., Vougioukalakis, G., Roman, C.N., Cantner, K., Bejelou, K., Bourbouli, M., Martin, J.F., 2011. Exploration of the Kolumbo Volcanic Ri Zone. In K.L.C. Bell and S.A. Fuller (eds.), New Frontiers in Ocean Exploration: E/V Nautilus 2010 Field Season. Oceanography 24, supplement, pp. 24-25. https://doi. 10.5670/oceanog.24.1.supplement

Carey, S., Bell, K.L.C., Sparks, R.S.J., Stinton, A., Ausubel, J., Phillips, B., Raineault, N., Siu, N., Fandel, C., Graham, O., Ramsingh, H., Blake, R., Auscavitch, S., Demopoulos, A., Rodrigue, K., 2014a. Impact of volcanic eruptions on the seafloor around Montserrat, West Indies. In: Bell, K.L.C., M.L. Brennan, and N.A. Raineault, eds. 2014. New Frontiers in Ocean Exploration: The E/V Nautilus 2013 Gulf of Mexico and Caribbean Field Season. Oceanography 27(1), supplement, 52 pp, https://doi.org/10.5670/oceanog.2014.supplement.01.

Carey, S., Bell, K.L., Ballard, R.D., Roman, C., Dondin, F., Miloslavich, P., Gobin, J., Seibel, B., Smart, C., Fuller, S., Siu, N., 2014b. Fluid/gas venting and biological communities at Kick'em Jenny submarine volcano, Grenada (West Indies). Oceanography 27, 38-41.

Carey, S., Ballard, R., Bell, K. L. C., Bell, R. J., Connally, P., Dondin, F. et al., 2014c. Cold seeps associated with a submarine debris avalanche deposit at Kick'em Jenny volcano, Grenada (Lesser Antilles). Deep-Sea Research Part I-Oceanographic Research Papers 93, 156– 160. https://doi.org/10.1016/j.dsr.2014.08.002

Carey, S., Bell, K. L.C., Roman, C., Dondin, F., Robertson, R., Gobin, J., Wankel, S., Michel, A.P.M., Amon, D.J., Marsh, L., Smart, C. Vaughan, I., Ball, B., Rodrigue, K.,

Haldeman, M., George, A., Ballard, R., 2015. Exploring Kick'em Jenny submarine volcano and the Barbados Cold Seep Province, Southern Lesser Antilles [in special issue: New Frontiers in Ocean Exploration: The E/V Nautilus 2014 Gulf of Mexico and Caribbean Field Season]. Oceanography 28 (1, Supplement), 38-39.

Carey, S., Sparks, R.S.J., Tucker, M.E., Robertson, L., Watt, S.F.L., Gee M., Hastie, A., Li, T., Barfod, D.N., Stinton, A., Raineault, N. and Ballard, R.B.D. 2019. The polygenetic Kahouanne Seamounts in the Northern Lesser Antilles Island Arc: Evidence for large-scale volcanic island subsidence. Marine Geology 419, 10646.

Cassidy, M., Taylor, R.N., Palmer, M.R., Cooper, R.J., Stenlake, C., Trofimovs, J., 2012. Tracking the magmatic evolution of island arc volcanism: Insights from a high-precision Pb isotope record of Montserrat, Lesser Antilles. Geochem. Geophys. Geosyst. 13, Q05003, doi:10.1029/2012GC004064.

Cassidy, M., Trofimovs, J., Palmer, M.R., Talling, P.J., Watt, S.F.L., Moreton, S.G., Taylor, R.N., 2013. Timing and emplacement dynamics of newly recognized mass flow deposits at ~8–12 ka offshore Soufrière Hills volcano, Montserrat: How submarine stratigraphy can complement subaerial eruption histories. Journal of Volcanology and Geothermal Research 253, 1-14.

Chiodini, G., Cioni, R., Frullani, A., Guidi, M., Marini, L., Prati, F., Raco, B., 1996. Fluid geochemistry of Montserrat Island, West Indies. Bull. Volcanol. 58, 380–392.

Christ, N., Immenhauser, A., Wood, R.A., Darwich, K., Niedermaya, A., 2015. Petrography and environmental controls on the formation of Phanerozoic marine carbonate hardgrounds. Earth-Science Reviews 151, 176–226.

Cooper, H.H., 1959. A hypothesis for the dynamic balance of freshwater and saltwater in a coastal aquifer. Journal of Geophysical Research 64, 461-467.

Coussens, M., Cassidy, M., Watt, S. F. L., Jutzeler, M., Talling, P. J., Barfod, D. et al., 2017. Long-term changes in explosive and effusive behaviour at andesitic arc volcanoes:

Chronostratigraphy of the Centre Hills Volcano, Montserrat. Journal of Volcanology and Geothermal Research 333–334, 15–35. https://doi.org/10.1016/j.jvolgeores.2017.01.003.

Darwin, C., 1874. The Structure and Distribution of Coral Reefs. Revised edition. London: Smith, Elder & Co. 1874.

Devas, R.P., 1974. History of the Island of Grenada, pp. 1498–1796, Carenage Press, St. George's, Grenada.

Dondin, F., Lebrun, J.F., Kelfoun, K., Fournier, N., Randrianasolo, A., 2012. Sector collapse at Kick'em Jenny submarine volcano (Lesser Antilles): Numerical simulation and landslide behavior. Bull. Volcanol. 74, 595–607.

Dravis, J., 1979. Rapid and widespread generation of Recent oolitic hardgrounds on a high energy Bahamian platform, Eleuthera bank, Bahamas. J. Sediment. Petrol. 49, 195–207.

Dupraz, C.R., P., R., Braissant, O., Decho, A.W., Norman, R.S., Visscher, P.T., 2009. Processes of carbonate precipitation in modern microbial mats. Earth Sci. Rev. 96, 141–162.

Farrell, J.W., Clemens, S.C., Gromet, P.L., 1995. Improved chronostratigraphic reference curve of late Neogene seawater $^{87}Sr/^{86}Sr$. Geology 23, 403–406.

Feuillet, N., Leclerc, F. Tapponnier,P., François Beauducel, F., Boudon,G., Le Friant, A. Deplus, C., Lebrun, J-F., Nercessian, A., Saurel, J-M., Clément, V., 2010. Active faulting induced by slip partitioning in Montserrat and link with volcanic activity: new insights from the 2009 GWADASEIS marine cruise data. Geophysical Research Letters 37, L00E15, https://dx.doi.org/10.1029/2010GL042556

Harford, C. L., Pringle, M. S., Sparks, R. S. J., Young, S. R., 2002. The volcanic evolution of Montserrat using $^{40}Ar/^{39}Ar$ geochronology. In T. H. Druitt & B. P. Kokelaar (Eds.), The eruption of the Soufrière Hills Volcano, Montserrat from 1995 to 1999 (Vol. 21, pp. 93–113). London, UK: Geological Society Memoirs. https://doi.org/10.1144/GSL.MEM.2002.021.01.05

Hatter, S.J., Palmer, M.R., Gernon, T.M., Taylor, R.N., Cole, P.D., Barfod, D.N., Coussens, M., 2018. The evolution of the Silver Hills volcanic center, and revised $^{40}Ar/^{39}Ar$ geochronology of Montserrat, Lesser Antilles, with implications for island arc volcanism. Geochemistry, Geophysics, Geosystems 19. https://doi.org/10. 1002/2017GC007053.

Hemmings, B., Whitaker, F., Gottsmann, J., Hughes, A., 2015. Hydrogeology of Montserrat, review and new insights. Journal of Hydrology: regional studies 3, 1-30.

Horwitz, E.P., Chiarizia, R., Dietz, M.L., 1992. A novel strontium-selective extraction chromatographic resin. Solvent Extr. Ion Exch. 10, 313–336.

Howarth, R.J., McArthur, J.M. (1997) Statistics for strontium isotope stratigraphy: A robust LOWESS fit to the marine Sr-isotope curve for 0 to 206 Ma, with look-up table for derivation of numeric age. Journal of Geology 105, 441–456.

Join, J-L., Folio, J-L., Robineau, B., 2005. Aquifers and groundwater within active shield volcanoes. Evolution of conceptual models in the Piton de la Fournaise volcano. Journal of Volcanology and Geothermal Research 147, 187– 201

Jones, G., Whitaker, F., Smart, P., Sanford, W. (2000) Numerical modelling of geothermal and reflux circulation in Enewetak Atoll: implications for dolomitization. J. Geochem. Explor. 69-70, 71–75.

Kameo, K., Shearer, M.C., Droxler, A.W., Mita, I., Watanabe, R., Sato, T., 2004. Glacial–interglacial surface water variations in the Caribbean Sea during the last 300 ky based on calcareous nannofossil analysis. Palaeogeography, Palaeoclimatology, Palaeoecology 212, 65– 76.

Kenedi, C.L, Sparks, R.S.J., Malin, P.E., Voight, B., Dean, S., Minshull, T., Paulatto, M., Peirce, C., Shalev, E., 2010. Contrasts in morphology and deformation offshore Montserrat: New insights from the SEA-CALIPSO marine cruise data. Geophysical Research Letters 37, L00E25, doi:10.1029/2010GL043925.

Kim K-Y., Park, E., Han W.S., 2010. Effect of a high permeable layer on hydraulic system in a coastal aquifer. SWIM21 - 21st Salt-Water Intrusion Meeting, Azores Portugal, 359- 362.

Konhauser, K.O., 1998. Diversity of bacterial iron mineralization. Earth Sci. Rev. 43, 91–121.

Kokelaar, B.P., 2002. Setting, chronology and consequences of the eruption of Soufrière Hills Volcano, Montserrat (1995-1999). *In* Druitt, T.H. and Kokelaar, B.P., The Eruption of the Soufrière Hills Volcano, Montserrat, From 1995 to 1999, Geological Society, London, Memoirs 21, 1–43. https://doi.org/10.1144/GSL.MEM.2002.021.01.02

Le Friant, A., Harford, C.L., Deplus, C., Boudon, G., Sparks, R.S.J., Herd, R.A., Komorowski, J.C., 2004. Geomorphological evolution of Montserrat (West Indies): importance of flank collapse and erosional processes. Journal of the Geological Society of London 161, 147-160.

Le Friant, A., Deplus, C., Boudon, G., Sparks, R.S.J., Trofimovs, J., Talling. P.J., 2009. Submarine deposition of volcaniclastic material from the 1995-2005 eruptions of Soufrière Hills Volcano, Montserrat. Journal of the Geological Society of London 166, 171-182.

Lewis, J., Coath, C., Pike, A., 2014. An improved protocol for $^{87}Sr/^{86}Sr$ by laser ablation multi-collector inductively coupled plasma mass spectrometry using oxide reduction and a customised plasma interface. Chemical Geology 390, 173-181.

Lindsay, J., Shepherd, J.B., Wilson, D., 2005. Volcanic and scientific activity at Kick'em Jenny submarine volcano 2001-2002: Implications for volcanic hazards in the southern Grenadines, Lesser Antilles. Nat. Hazard 34, 1–24.

Macgregor, A.G., 1938. The Royal Society Expedition to Montserrat, B.W.I. The volcanic history and petrology of Montserrat with observations on Mt Pele, in Martinique. Philosophical Transactions of the Royal Society of London B229, 1-90.

Malone, M.J., Slowey, N.C., Henderson, G.M., 2001. Early diagenesis of shallow-water periplatform carbonate sediments, leeward margin, Great Bahama Bank (Ocean Drilling Program Leg 166). GSA Bull. 113, 881–894.

McArthur, J.M., Howarth, R., Shields, G., 2012. Strontium isotope stratigraphy. In: the Geologic Time-Scale. Elsevier pp. 127–144.

McArthur, J.M., Rio, D., Massari, F., Castradori, D., Bailey, T.R., Thirlwall, M., Houghton, S., 2006. A revised Pliocene record for marine $^{87}Sr/^{86}Sr$ used to date an interglacial event recorded in the Cockburn Island Formation, Antarctic Peninsula. Palaeogeography, Palaeoclimatology, Palaeoecology 242, 126–136.

McKenzie, J.A., Bernoulli, D.,1982. Geochemical variations in Quaternary hardgrounds from the Hellenic Trench region and possible relationship to their tectonic setting. Tectonophysics. 86: 149-157. https//doi.10.1016/0040-1951(82)90065-8

Melim, L.A., Swart, P.K., Maliva, R.G., 1995. Meteoric-like fabrics forming in marine waters: Implications for the use of petrography to identify diagenetic environments. Geology 23, 755-758.

Melim, L.A., Westphal, H., Swart, P.K., Eberli, G.P., Munnecke, A., 2002. Questioning carbonate diagenetic paradigms: evidence from the Neogene of the Bahamas. Marine Geology 185, 27-53.

Milliman, J.D., 1974. Marine Carbonates. Springer-Verlag, Berlin.

Moore, J.G., Fornari, D.J., 1984. Drowned reefs as indicators of the rate of subsidence of the Island of Hawaii. Journal of Geology, 92, 752-759.

Murray, J., Renard, A.F., 1891. Report on deep-sea deposits. Report on the Scientific Results of the Voyage of H.M.S. Challenger During the Years 1873–76. Neill and Co., Edinburgh.

Nier, A.O., 1938. The isotopic constitution of strontium, barium, bismuth, thallium and mercury. Physical Review 54, 275–78.

Noé, S., Titschack, J., Freiwald, A., Dullo, W.-C., 2006. From sediment to rock: diagenetic processes of hardground formation in deep-water carbonate mounds of the NE Atlantic. Facies 52, 183–208.

Nomikou, P., Carey, S., Papanikolaou, D., Croff Bell, K., Sakellariou, D., Alexandri, M., Greece. Global and Planetary Change, 90-901, 135-151.

Perri, E., Tucker, M.E., Słowakiewicz, M., Whitaker, F., Bowen, L., Perrotta, I., 2018. Carbonate and silicate biomineralization in a hypersaline microbial mat (Mesaieed Sabkha, Qatar): roles of bacteria, EPS and viruses. Sedimentology, 65, 1213-1245.

Poux, B., Brophy, P., 2012. Geothermal exploration on the island of Montserrat, Caribbean. GRC Transactions, 36, 737–744.

Rea, W.J., 1974. The volcanic geology and petrology of Montserrat, West Indies. Journal of the Geological Society, London 130, 341–366.

Rebelo, A.C., Rasser, M., Kroh, A., Johnson, M.E., Melo, C., Ramalho, R.S., Uchman, A., Zanon, V., Silva. L., Neto, A., Berning, B., Cachão, M., Ávila, S., 2015. Rocking around a volcanic island shelf: Neogene rhodolith beds from Malbusca, Santa Maria Island (Azores, NE Atlantic). Facies 62, 22-31.

Russell W., Papanastassiou D., Tombrello T. 1978. Ca isotope fractionation on the Earth and other solar system materials. Geochimica et Cosmochimica Acta 42, 1075–90.

Ryan, G.A., Peacock, J.R., Shalev, E., Rugis, J., 2013. Montserrat geothermal system: A 3D conceptual model. Geophysical Research Letters 40, 1-6.

Schlager, W., James, N.P., 1978. Low-magnesian calcite limestones forming on the deep seafloor, Tongue of the Ocean, Bahamas. Sedimentology 25, 675–702.

Schroeder, T., John, B., Frost, B.R., 2002. Geologic implications of seawater circulation through peridotite exposed at slow-spreading mid-ocean ridges. Geology 30, 367–370.

Shepherd, J. B., Robson, G.R., 1967. The source of the T-phase recorded in the Eastern Caribbean on October 24, 1965. Bull. Seismol. Soc. Am. 57, 227–234.

Shinn, E.A., 1969. Submarine lithification of Holocene carbonate sediments in the Persian Gulf. Sedimentology 12, 109–144.

Sigurdsson, H., Shepherd, J.B., 1974. Amphibole-bearing basalts from the submarine volcano Kick'em Jenny in the Lesser Antilles arc. Bull. Volcanol. 28, 891–910.

Sigurdsson, H., Carey, S., Wilson, D., 2006. Debris Avalanche Formation at Kick'em Jenny Submarine Volcano, 66 pp., World Scientific, Hackensack, N. J.

Steiger, R., Jäger E., 1977. Subcommission on Geochronology: Convention on the use of decay constants in geo-and cosmochronology. Earth and Planetary Science Letters 36, 359–62.

Stoddart, D.R., 1976. Darwin, Lyell, and the geological significance of coral reefs. British Journal for the History of Science 9, 199–218.

Swart, P., 2015. The geochemistry of carbonate diagenesis: The past, present and future. Sedimentology 62, 1233–1304.

Thirlwall, M.F., 1991, Long-term reproducibility of multicollector Sr and Nd isotope ratio analysis. Chemical Geology 94, 85-104.

Thompson, G., Bowen, V.T., Melson, W.G., Cifelli, R., 1968. Lithified carbonates from the deep-sea of equatorial Atlantic. J. Sediment. Petrol. 38, 1305–1312.

Trofimovs, J., Foster, C., Sparks, R.S.J., Loughlin, S., Le Friant, A., Deplus, C., Porritt, L., Christopher, T., Luckett, R., Talling, P.J., Palmer, M.R., Le Bas, T., 2012. Submarine pyroclastic deposits formed during the 1 20th May 2006 dome collapse of the Soufrière Hills volcano. Montserrat. Bulletin of Volcanology 74, 395-401.

Tucker, M.E., 1993. Carbonate diagenesis and sequence stratigraphy. In: Sedimentology Review (Ed. V.P. Wright) 1, 51-72.

Tucker, M.E., Wright, V.P., 1990. Carbonate Sedimentology. Blackwell Science. Oxford.

van der Kooij, B., Immenhauser, A., Steuber, T., Bahamonde, J.R., Merino Tomé, O., 2010. Precipitation mechanisms of volumetrically important early marine carbonate cement volumes in deep-slope settings. Sedimentology 57, 1491–1525.

van der Land, C., Mienis, F., De Haas, H., Frank, N., Swennen, R., Van Weering, T.C.E., 2010. Diagenetic processes in carbonate mound sediments at the south-west Rockall Trough margin. Sedimentology 57, 912–931.

Wadge, G., Voight, B., Sparks, R.S.J., Cole, P., Loughlin, S.C., 2014. An overview of the eruption of Soufrière Hills Volcano from 2000-2010. In: The Eruption of the Soufrière Hills Volcano, Montserrat from 2000-2010 edited by Wadge, G., Robertson, R.A.E. and Voight, B. Geological Society Memoir 39, 1-40.

Watt, S.F.L., Talling, P.J., Vardy, M.E., Masson, D.G., Henstock, T.J., Hühnerbach, V., Minshull, T.A., Urlaub, M., Lebas, E., Le Friant, A., Berndt, C., Crutchley, G.J., Karstens, J., 2012. Widespread and progressive seafloor-sediment failure following volcanic debris avalanche emplacement: landslide dynamics and timing offshore Montserrat, Lesser Antilles. Mar. Geol. 323–325, 69–94. https//doi:10.1016/ j.margeo.2012.08.002

Watt, S.F.L., Jutzeler, M., Talling, P.J., Carey, S.N., Sparks, R.S.J., Tucker, M.E, Stinton, A.J., Fisher, J.K., Wall-Palmer, D., Hühnerbach, V., Moreton, S.G., 2015. New insights into landslide processes around volcanic islands from Remotely Operated Vehicle (ROV) observations offshore Montserrat. Geochemistry, Geophysics, Geosystems 16, 2240-2261.

Webster, J.M., Braga, J.C., Clague, D.A., Gallup, C., Hein, J.R., Potts, D., Renema, W., Riding, R., Riker-Coleman, K., Silver, E., Wallace, L.M., 2009. Coral reef evolution on rapidly subsiding margins. Global and Planetary Change 66, 129–148.

Whitaker, F.F., Smart, P.L., 1990. Active circulation of saline ground waters in carbonate platforms: Evidence from the Great Bahama Bank. Geology 18, 200-203.

Zellmer, G.F., Hawkesworth, C.J., Sparks, R.S.J., Thomas, L.E., Harford, C.L., Brewer, T.S., Loughlin, S.C., 2003. Geochemical evolution of the Soufrière Hills Volcano, Montserrat, Lesser Antilles Volcanic Arc. Journal of Petrology 44, 1349-1374.

Captions to figures

Fig. 1 Map showing the location of Montserrat island in the northern Lesser Antilles and the bathymetry of the surrounding seafloor. Principal volcanic centres on Montserrat are marked by red triangles. Faults are indicated based on Feuillet et al. (2010) and on interpretation of seismic reflection data in Watt et al. (2012). The inset map shows the location of the study region within the Lesser Antilles. Locations of seismic reflection lines from previous studies are indicated by the blue and green lines that cross the Kahouanne valley.

Fig. 2. Maps showing the location of carbonate samples from a) Kick'em Jenny submarine volcano area in the southern Lesser Antilles and b) Kolumbo submarine volcano and other seamounts northeast of the Santorini volcanic complex in the southern Aegean Sea. Sample localities are shown with red stars. Insert map in the Kolumbo figure shows the location of the sampling area relative to Santorini.

Fig. 3. High-resolution multibeam map of the area southeast, south, and east of the island of Montserrat. Carbonate samples used in the study are shown by red stars. Depth key is in the lower right-hand corner of the figure. Irregular hummocky seafloor to the south and east of Montserrat consists of large-scale debris avalanche deposits.

Fig. 4. Montserrat SW Nearshore. a) Collecting sample NA037-029 at 188 m depth from a low cliff. b) Well-indurated volcaniclastic-bioclastic pack-grain-rudstone with volcanic clasts coated by coralline algae. c) Micrite-filled sponge borings cutting shell and adjacent sediment indicating two phases cementation (thin-section, ppl). d) Grains cemented by isopachous fibrous calcite crust (thin-section, ppl).

Fig. 5. Montserrat SW Nearshore. a) Site of sample NA037-033 at 292 m. b) Cemented slope sediment consisting of volcanic clasts encrusted with calcareous algae, in a bioclastic volcaniclastic pack-grain-rudstone with shell fragments. c) Encrustation of volcanic clast with foraminifera, serpulids and calcareous red algae (thin-section, ppl). d) Peloids between grains, probably microbial (thin-section, ppl). e) Volcanic and bioclastic grains cemented by isopachous calcite fringe (thin-section, xp). f) Isopachous calcite cement fringe around bioclasts (thin-section, ppl).

Fig. 6. Montserrat SW Offshore, sample NA037-025, depth 806 m. a) Cemented bioclastic-volcaniclastic grainstone. b) Bioclasts, intragranular peloidal sediment, fringing calcite cement (thin-section, ppl). c) Isopachous fibrous calcite cement around grains (thin-section, ppl). d) SEM-BSE micrograph of calcite cement around bioclasts and aragonite cement within gastropod (upper left).

Fig. 7. Montserrat SW Offshore. a) Collecting sample NA037-026, depth 823 m. b), c) Bioclastic-volcanic pack-grain-rudstone with enrusted volcanic grains (thin-section, ppl). d) Encrustation of volcanic clast by foraminifera, coralline algae, microbialite with filaments and serpulid (thin-section, ppl). e) Gastropod shell (formerly aragonite) dissolved out; whorl filled with calcite spar cement (thin-section, ppl).

Fig. 8. Kick'em Jenny, off Grenada. a) Sampling the seafloor crust. b) Sample NA039-071, 1956 m depth. Pelagic lime mudstone with large burrows. c) Intraclasts and pellets of lime mud within burrow cavity. Patchy calcite cement fringes around clasts (thin-section, ppl). d) Ostracod filled by microfossiliferous lime mud; patchy bladed-fibrous calcite cement around shells (thin-section, ppl).

Fig. 9. Kick'em Jenny sample NA039-035, depth 172 m. a) Volcaniclastic material with patches of dark lime mud, some of which may have infiltrated cavities. Note cavities filled with peloids (thin-section, ppl). b) Close-up of micritic peloids, probably of microbial origin, within cavities (thin-section, ppl).

Fig. 10. Kolumbo seamount. a) Sample NA007-001 depth 200 m – a pelagic limestone with fine volcanic material, with two phases of sponge boring, 2nd phase empty, and bivalve shell (thin-section, ppl). b) Collecting sample NA007-022, depth 194 m, with several crust layers. c), d) NA007-022 A complex volcaniclastic limestone calcareous alga with cavities (likely sponge borings) lined by a thin calcite cement crust, followed by an influx of pelagic sediment. Empty sponge borings from a later phase of boring (thin-section, ppl).

Fig. 11. Kolumbo seamount. a) Collecting sample NA007-045, depth 128 m. b), c), d) Loose coralline red algal framework with fine volcaniclastic-bioclastic material partly filling growth cavities. (b), c) thin-section, ppl; d) (xp).

Fig. 12. Carbon and oxygen isotope cross-plot (‰ VPDB) for crust samples and for samples from the geothermal well Mon3 and Roche's Bluff. Sample names are given on the figure for values plotting outside the marine area (i.e. positive $\delta^{18}O$ and $\delta^{13}C$). Also shown are the positions of the $\delta^{18}O$ values (but ‰ VSMOW) for geothermal and spring water from Hemmings et al. (2015) and Chiodini et al. (1996) respectively, and for fresh and altered SHV andesite from Zellmer et al. (2003).

Fig 13 – Schematic model for formation of slope crusts on a seamount developed through precipitation of carbonate from seawater entering the volcanic edifice through ocean currents, waves and storms, and seawater drawn in through Kohout convection.

Fig. 1

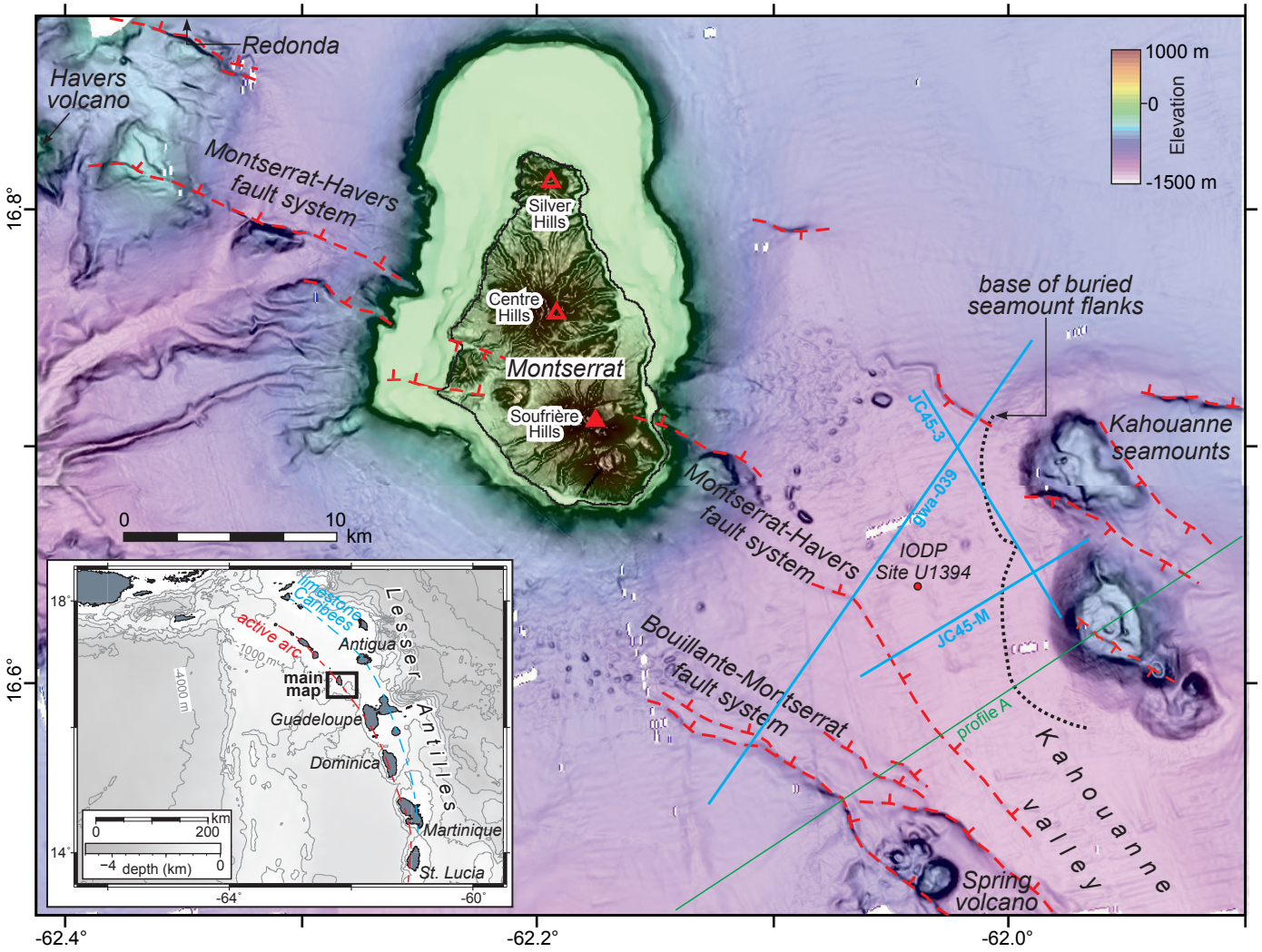
Redonda
Havers volcano
Montserrat-Havers fault system
Silver Hills
Centre Hills
Montserrat
Soufrière Hills
1000 m
0
-1500 m
Elevation
base of buried seamount flanks
Kahouanne seamounts
JC45-3
gwa-039
IODP Site U1394
JC45-M
Montserrat-Havers fault system
Bouillante-Montserrat fault system
profile A
Kahouanne valley
Spring volcano
0
10
km
16.8°
16.6°
-62.4°
-62.2°
-62.0°
inset map
active arc
limite Caraïbes
Lesser Antilles
Antigua
Guadeloupe
Dominica
Martinique
St. Lucia
1000 m
4000 m
km
0
200
−4
depth (km)
0
18°
14°
-64°
-60°

A.

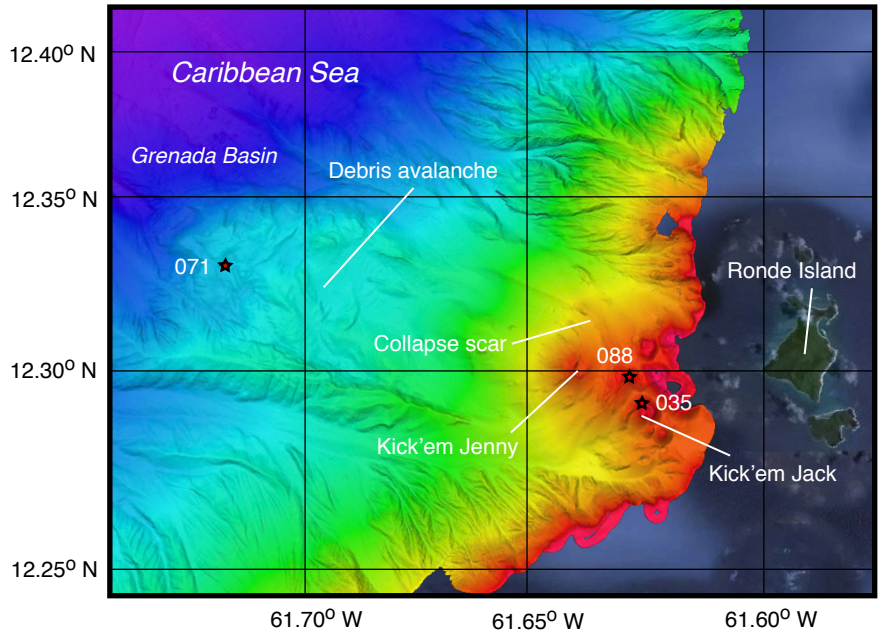
Caribbean Sea
Grenada Basin
Debris avalanche
071
Ronde Island
Collapse scar
088
035
Kick'em Jenny
Kick'em Jack
12.40° N
12.35° N
12.30° N
12.25° N
61.70° W
61.65° W
61.60° W

B.

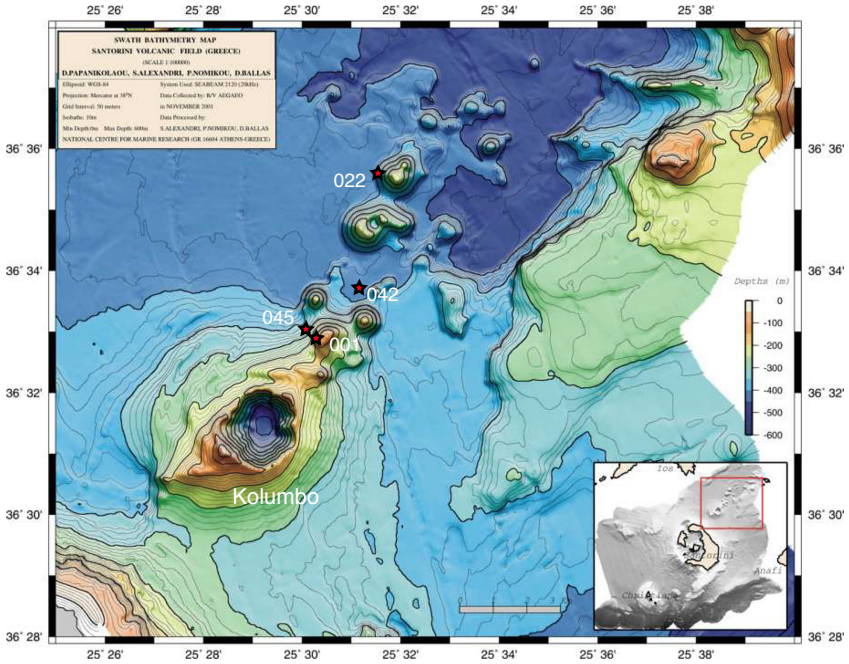
SWATH BATHYMETRY MAP
SANTORINI VOLCANIC FIELD (GREECE)
D.PAPANIKOLAOU, S.ALEXANDRI, P.NOMIKOU, D.BALLAS
022
042
045
001
Kolumbo
Depths (m)
0
-100
-200
-300
-400
-500
-600
25° 26'
25° 28'
25° 30'
25° 32'
25° 34'
25° 36'
25° 38'
36° 36'
36° 34'
36° 32'
36° 30'
36° 28'

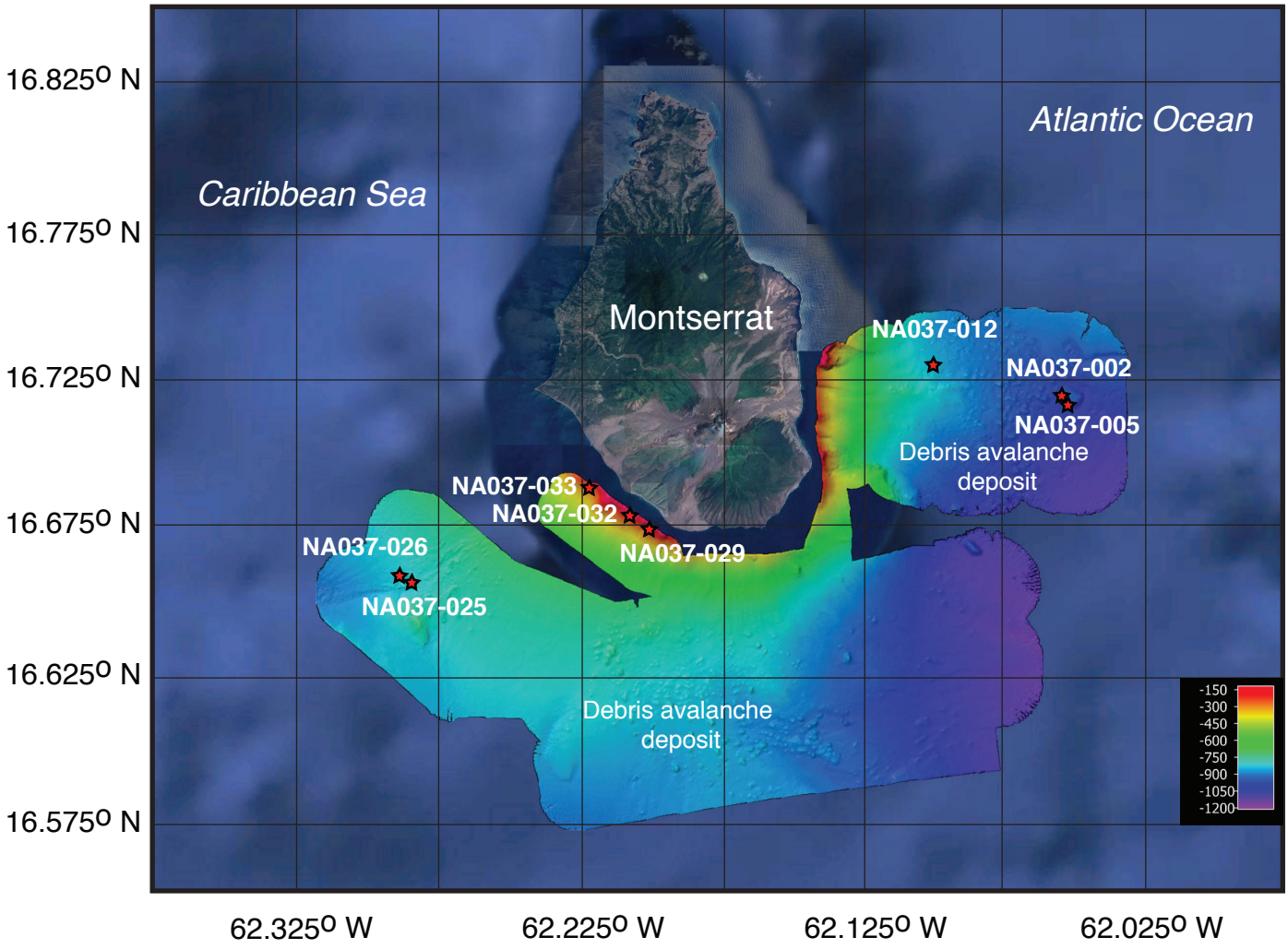
16.825° N
16.775° N
16.725° N
16.675° N
16.625° N
16.575° N
62.325° W
62.225° W
62.125° W
62.025° W
Caribbean Sea
Atlantic Ocean
Montserrat
NA037-012
NA037-002
NA037-005
Debris avalanche deposit
NA037-033
NA037-032
NA037-029
NA037-026
NA037-025
Debris avalanche deposit
-150
-300
-450
-600
-750
-900
-1050
-1200

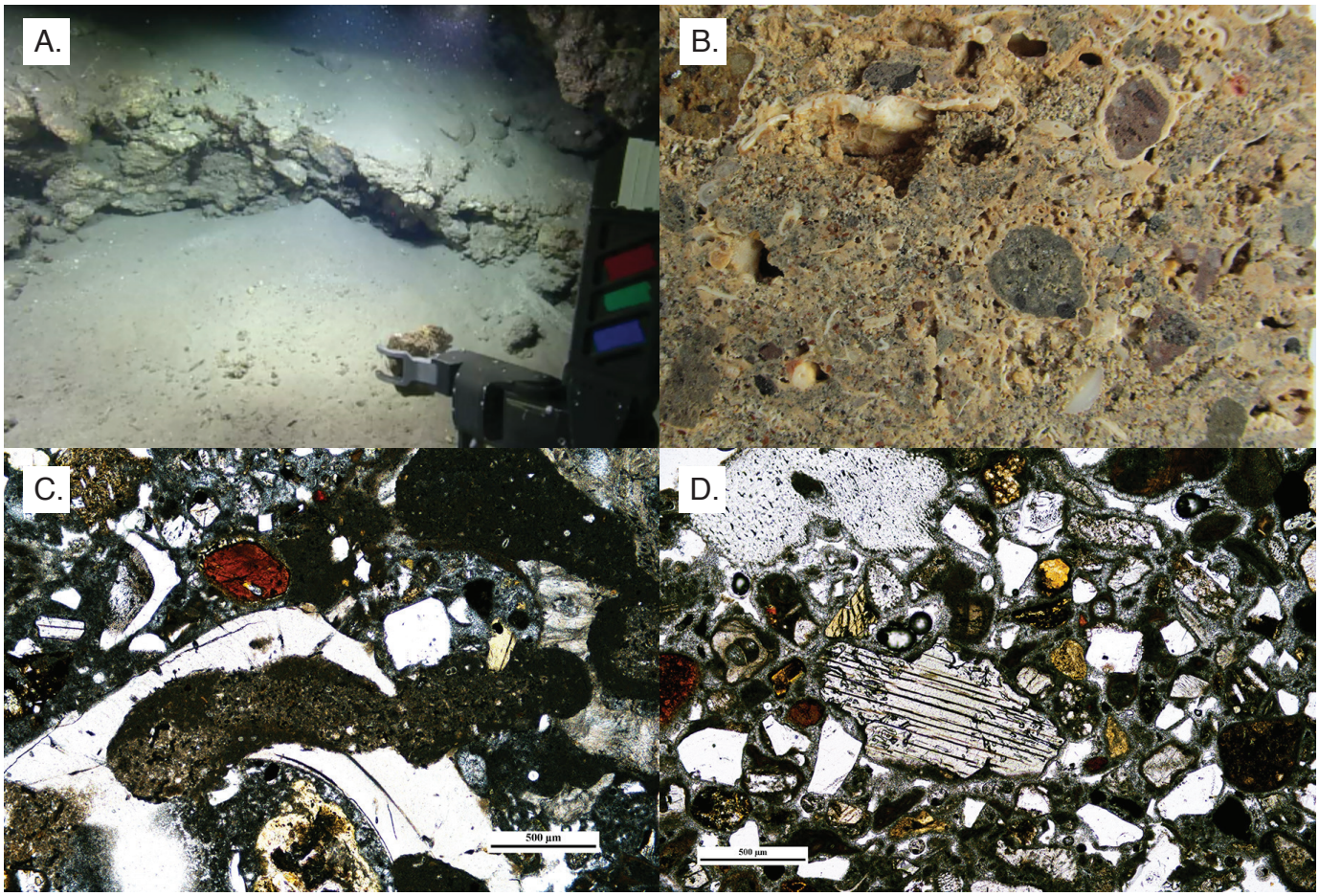
A.
B.
C.
500 µm
D.
500 µm

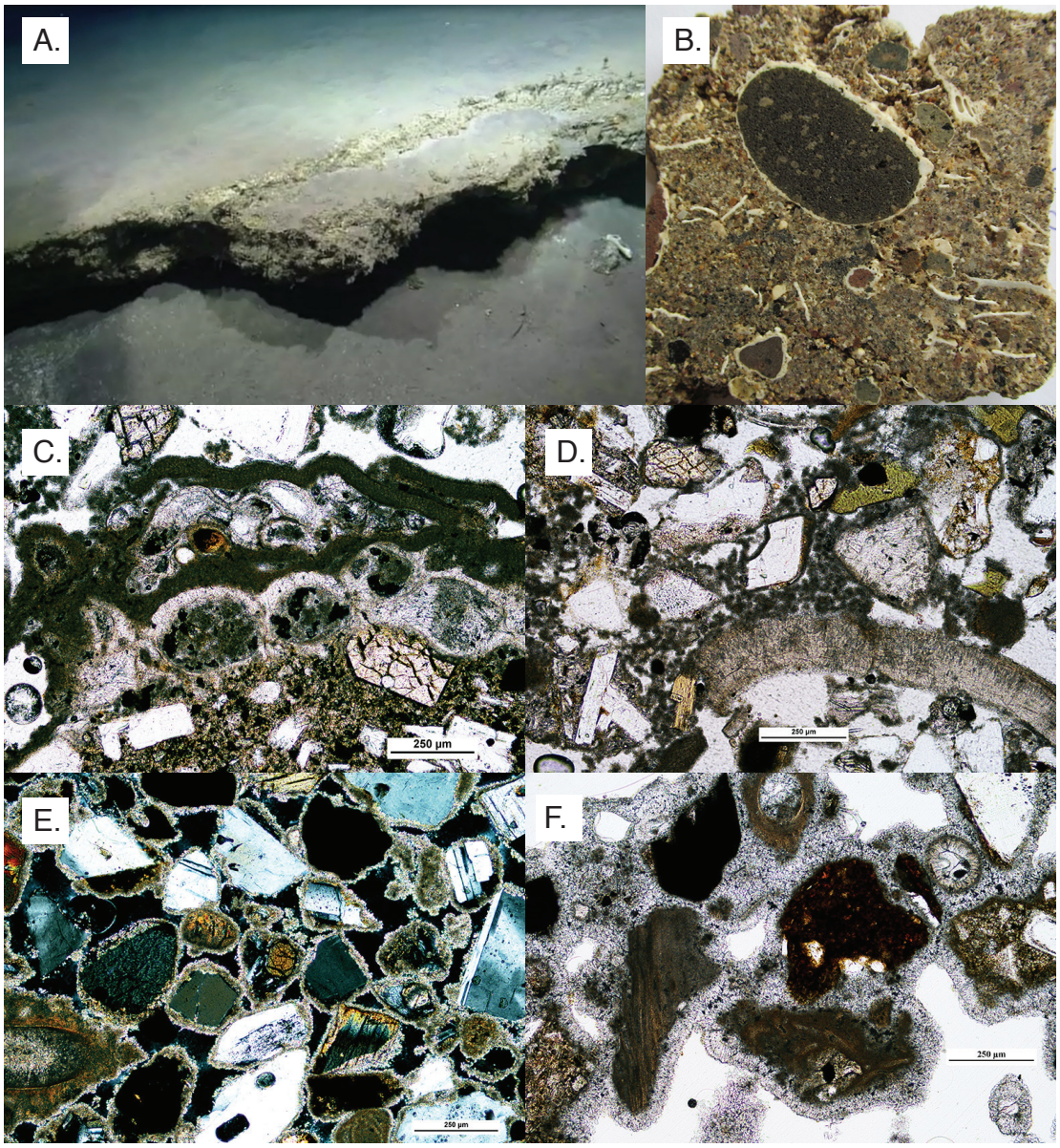
A.
B.
C.
250 µm
D.
250 µm
E.
250 µm
F.
250 µm

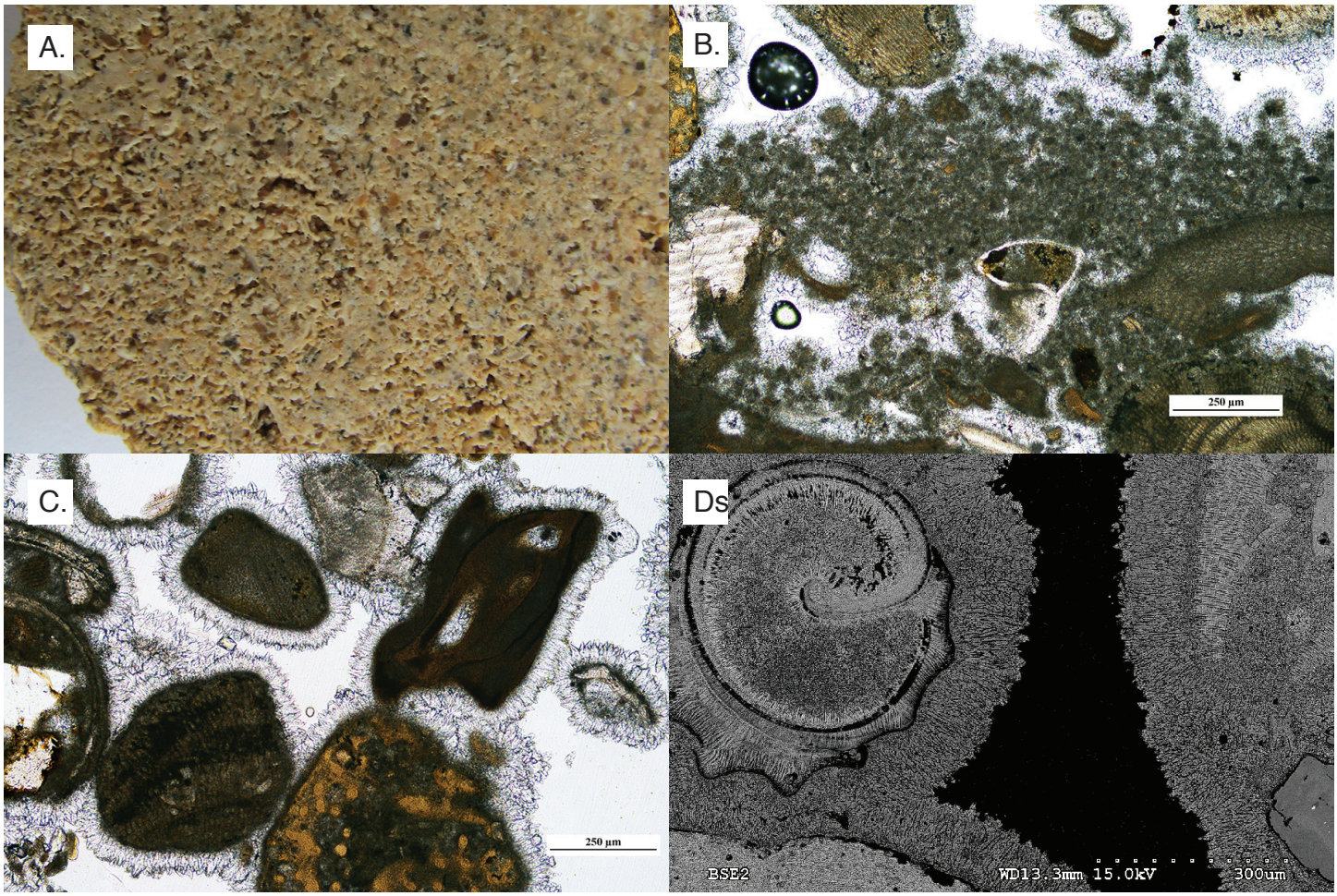
A.
B.
250 µm
C.
250 µm
Ds
BSE2
WD13.3mm 15.0kV
300um

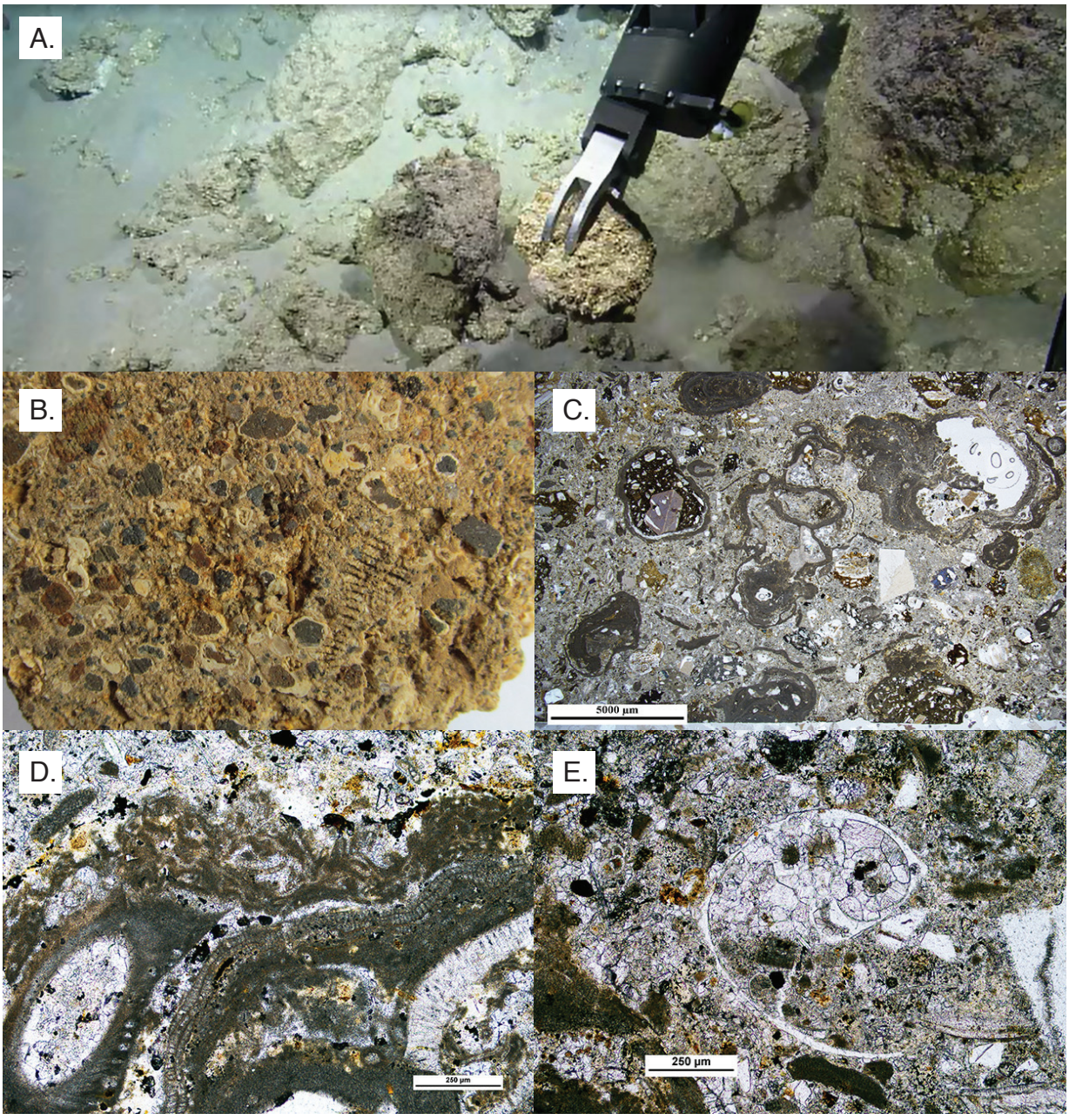
A.
B.
C.
5000 µm
D.
250 µm
E.
250 µm

Fig. 8

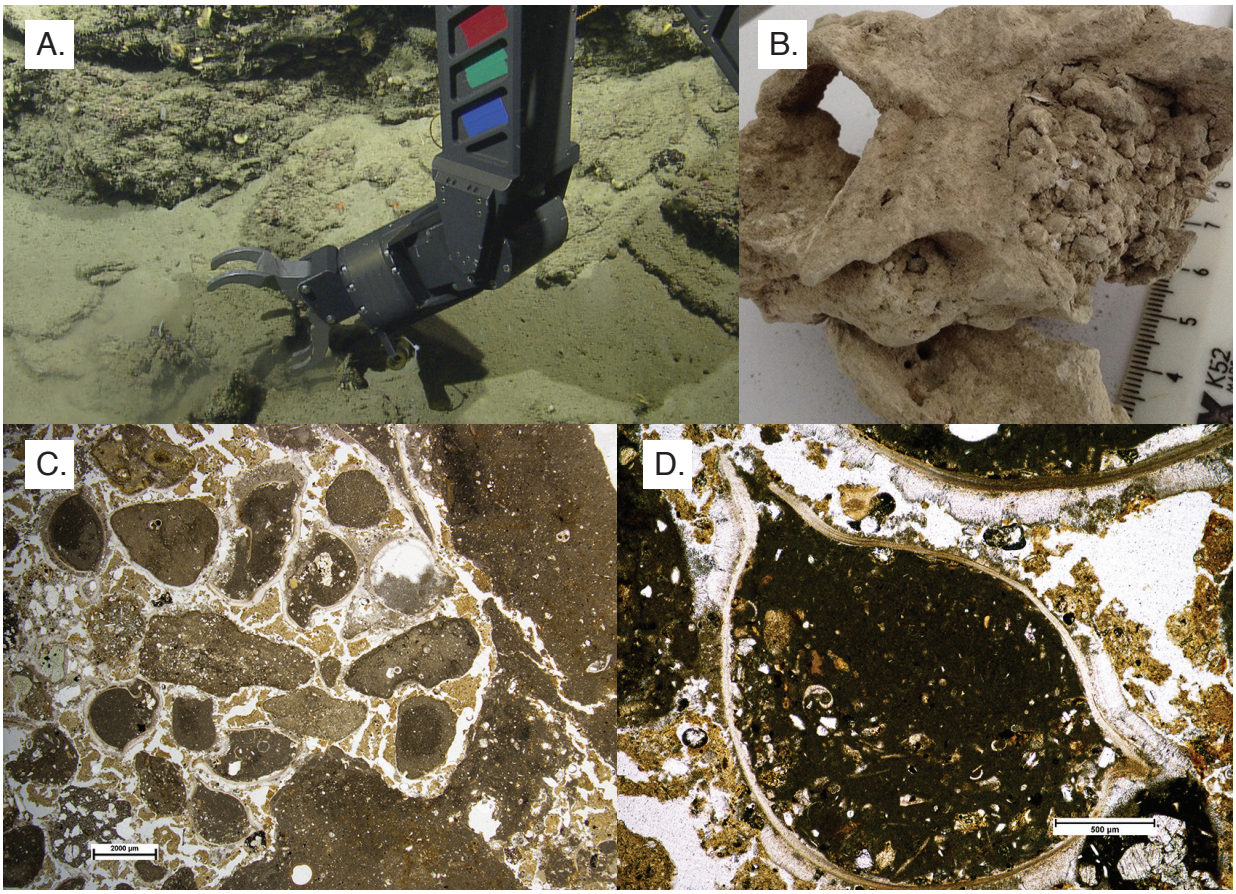

Fig. 9

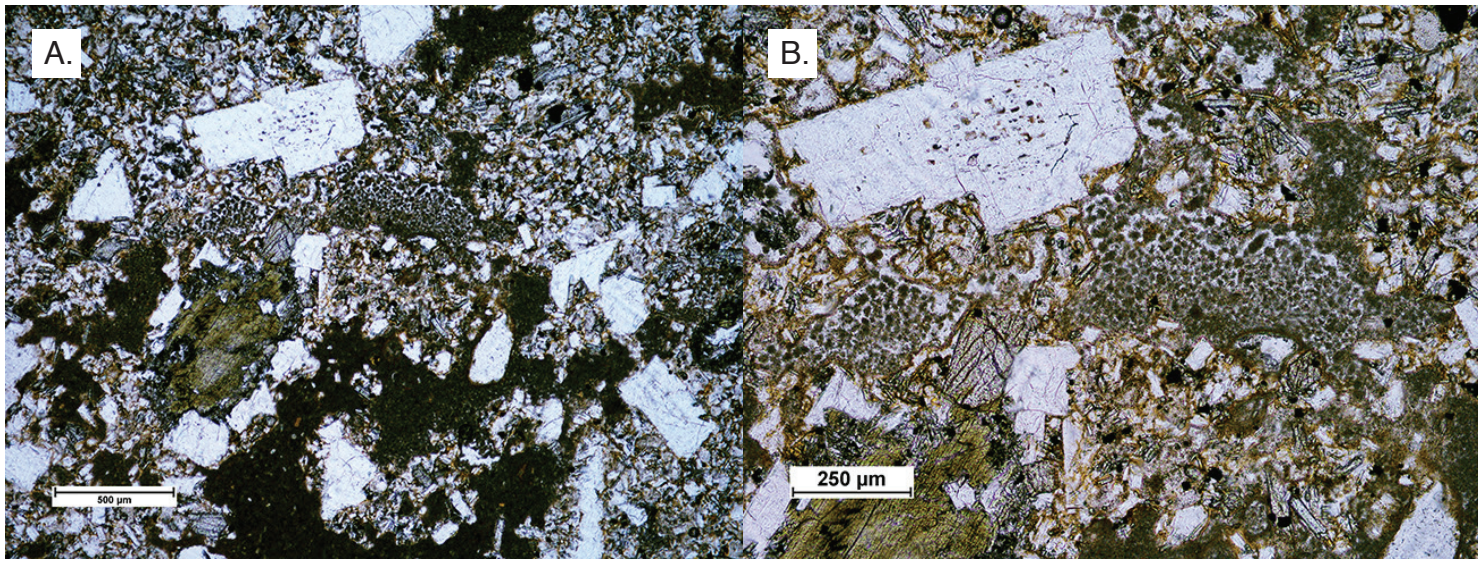

Fig. 10

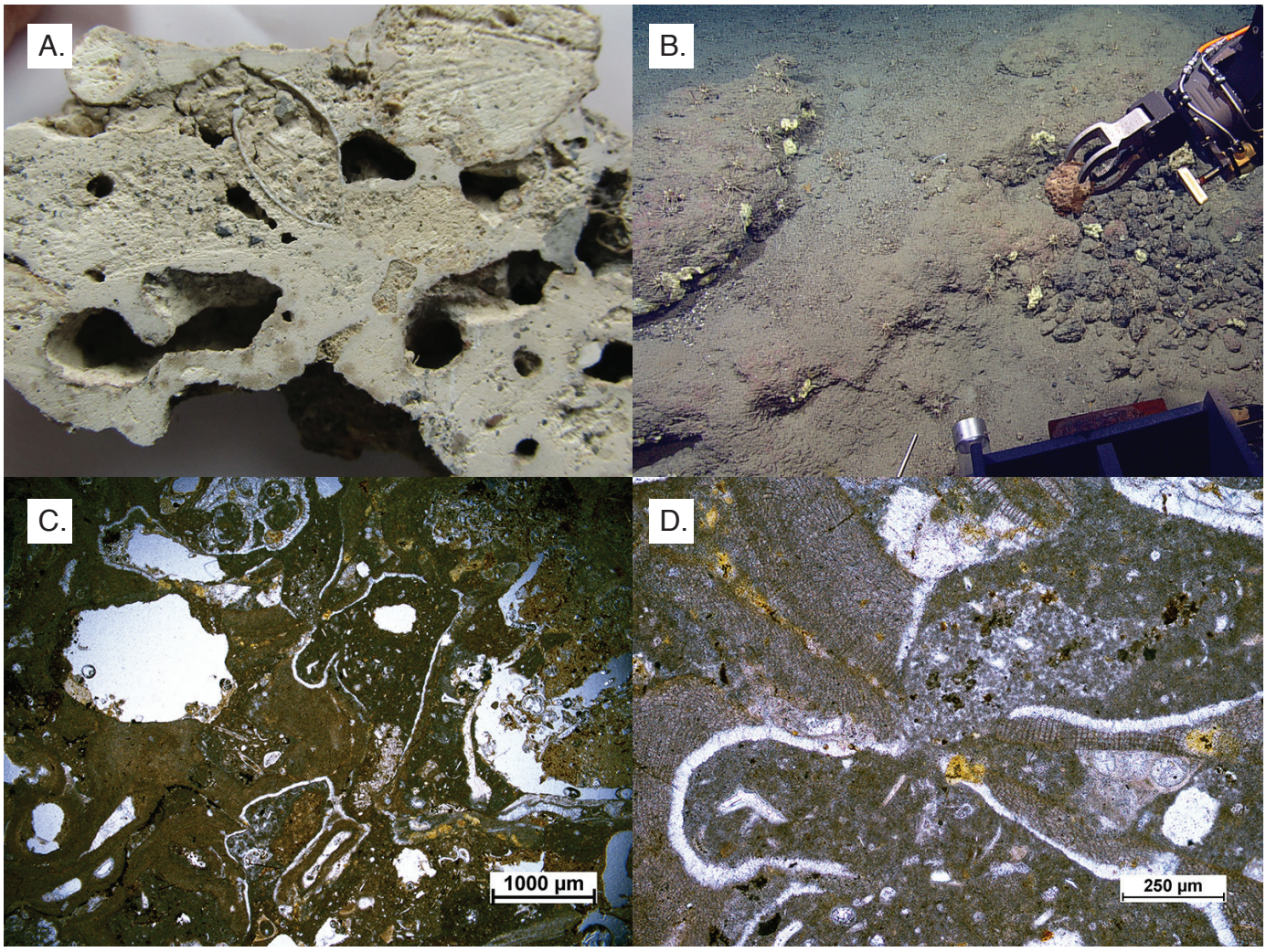

Fig. 11

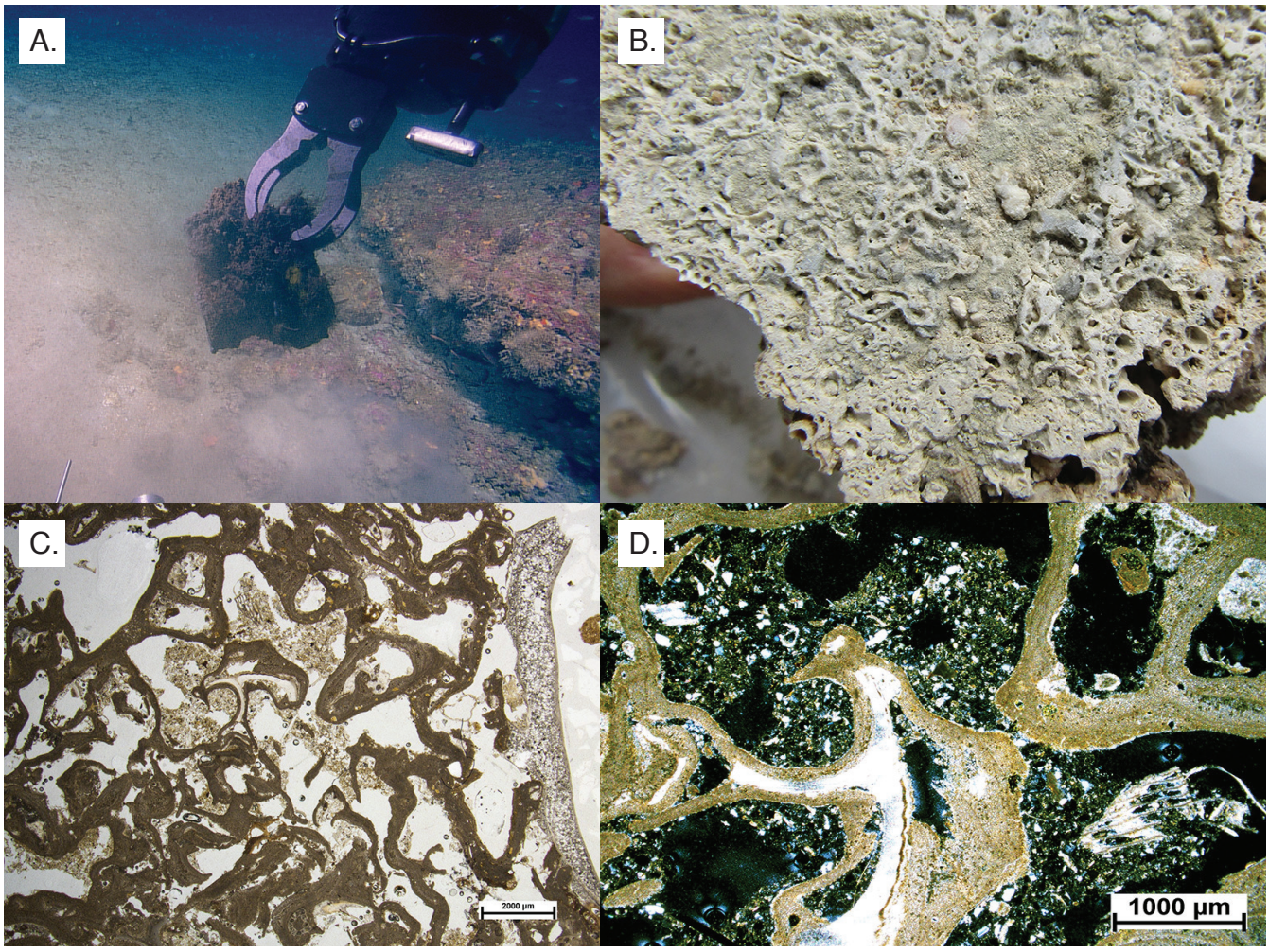

Fig. 12

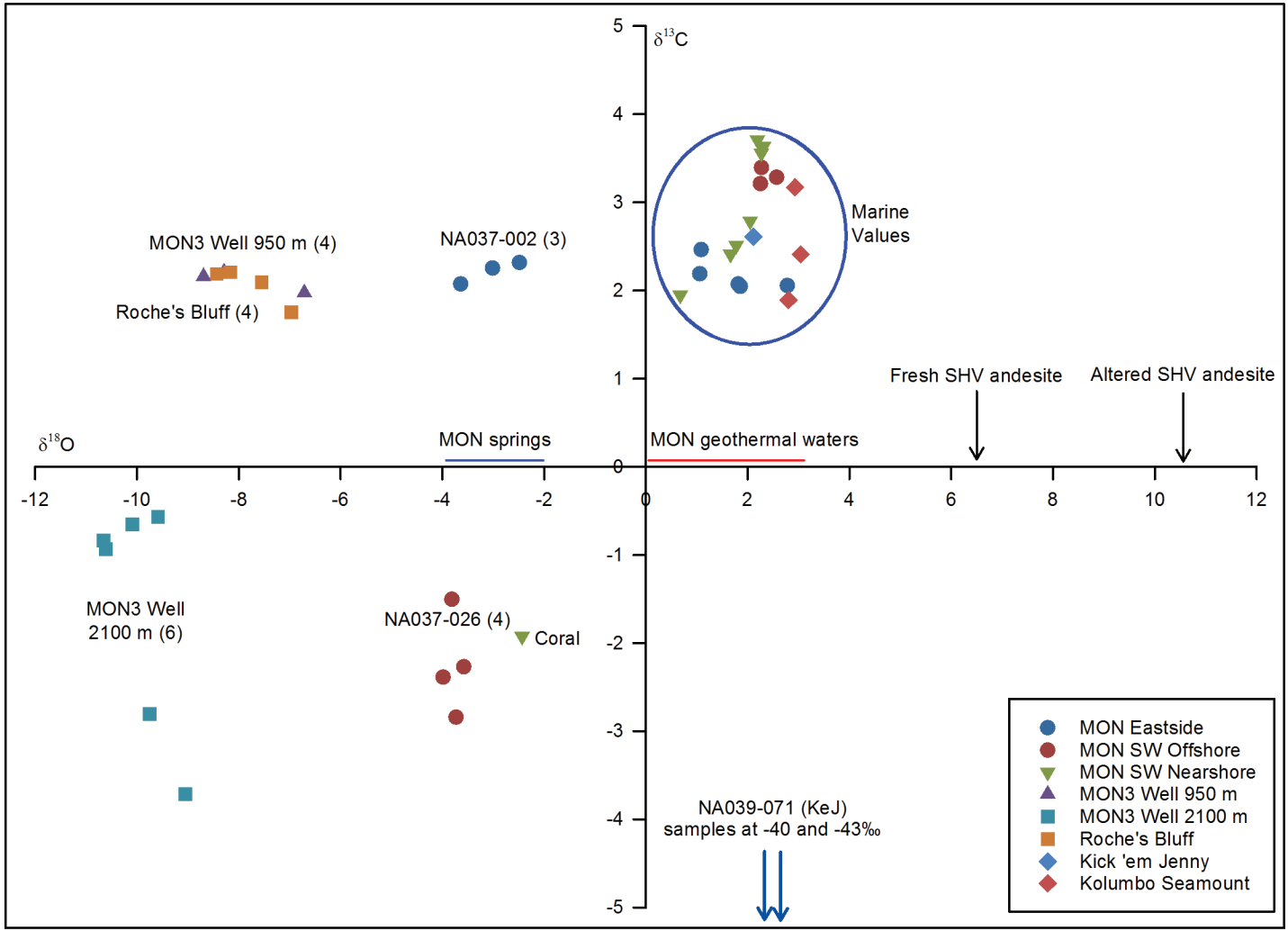
δ13C
δ18O
Marine Values
MON3 Well 950 m (4)
Roche's Bluff (4)
NA037-002 (3)
Fresh SHV andesite
Altered SHV andesite
MON springs
MON geothermal waters
MON3 Well 2100 m (6)
NA037-026 (4)
Coral
NA039-071 (KeJ) samples at -40 and -43‰
MON Eastside
MON SW Offshore
MON SW Nearshore
MON3 Well 950 m
MON3 Well 2100 m
Roche's Bluff
Kick 'em Jenny
Kolumbo Seamount

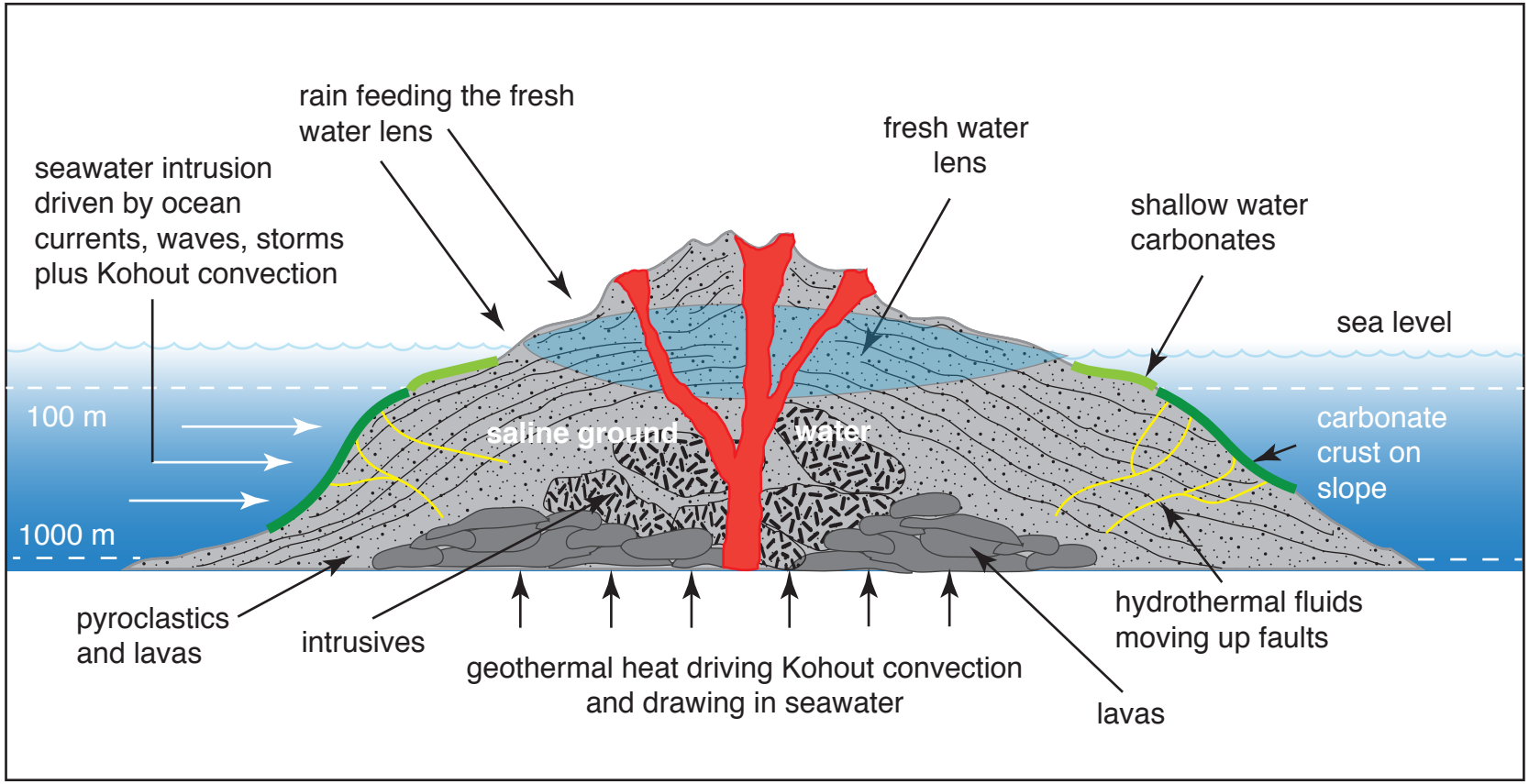
rain feeding the fresh water lens
fresh water lens
seawater intrusion driven by ocean currents, waves, storms plus Kohout convection
shallow water carbonates
sea level
100 m
saline ground
water
carbonate crust on slope
1000 m
pyroclastics and lavas
intrusives
geothermal heat driving Kohout convection and drawing in seawater
hydrothermal fluids moving up faults
lavas

Table 1. Samples of carbonate crusts from Nautilus cruises and Montserrat Geothermal Well

Area	Sample	Dive No.	Latitude degrees	minutes		Longitude degrees	minutes		Depth (m)	Shipboard Description
Montserrat	NA037-002	H1308	16	43.1221	N	62	3.3058	W	975	highly indurated carbonate with small lithic fragments
Caribbean	NA037-005	H1308	16	43.1424	N	62	3.27918	W	942	indurated foram-pteropod carbonate sediment with volcanic fragments
	NA037-012	H1308	16	43.8094	N	62	6.10538	W	840	bioclastic limestone
	NA037-025	H1309	16	39.4697	N	62	17.1064	W	806	yellow-white bioclastic grainstone with minor lithic
	NA037-026	H1309	16	39.4811	N	62	17.3912	W	823	white carbonate rock with encrusters
	NA037-029	H1309	16	40.5111	N	62	12.1067	W	188	bioclastic/volcaniclastic pack-rudstone with coated grains
	NA037-032	H1309	16	40.7931	N	62	12.4822	W	179	sample from metre-scale block of coral
	NA037-033	H1309	16	41.2414	N	62	13.3628	W	292	poorly sorted bioclastic grainstone with encrusters
Roche's Bluff	RB 1,2,3,4		16	41.8660	N	62	8.7050	W		coralgal-foram limestone + volcanic grains
Geothermal Well-3			16	43.7700	N	62	12.3970	W	930	planktic foraminiferal limestone
			16	43.7700	N	62	12.3970	W	950	bioclastic foram-coralgal limestone
			16	43.7700	N	62	12.3970	W	1198	bioclastic limestone
			16	43.7700	N	62	12.3970	W	2015	bioclastic foraminiferal limestone
			16	43.7700	N	62	12.3970	W	2016	coralliferous limestone
Hellenic Arc	NA007-001	H1103	36	32.5675	N	25	30.9119	E	200	dark brown, coralline-encrusted carbonate with cm-sized holes
Mediterrean	NA007-022	H1106	36	35.4636	N	25	31.9237	E	194	bio-encrusted (black crust, red crust, sponges, worms)
	NA007-045	H1107	36	32.9598	N	25	30.3470	E	128	clast from near top of cone 58
Kick'em Jenny	NA039-071	H1322	12	20.1605	N	61	43.7479	W	1956	partially indurated sediment with burrows
Caribbean	NA039-035	H1317	12	17.3905	N	61	37.4524	W	172	20 cm-sized rock encrusted with brown highly-indurated carbonate

Table 2. Stable carbon and oxygen isotope data for samples from Montserrat, Kick 'em Jenny Grenada, and Kolumbo Seamount, Mediterranean.

	δ^{13}C PDB	δ^{18}O PDB		interpretation
Montserrat SW Nearshore				
NA037-029A	3.56	2.27		marine
NA037-029B	3.63	2.3		marine
NA037-029C	3.57	2.18		marine
NA037-029-1	2.79	2.05		marine
NA037-032.1	-1.92	-2.44	coral	vital
NA037-032.2	1.95	0.67	serpulid	marine
NA037-033A	3.71	2.19		marine
NA037-033B	3.63	2.31		marine
NA037-033C	2.51	1.78	biocrust	marine
NA037-033D	2.41	1.66	biocrust	marine
Montserrat SW Offshore				
NA037-025A	3.28	2.57		marine
NA037-025B	3.21	2.25		marne
NA037-025.1	3.39	2.27		marine
NA037-026A	-2.39	-3.99		altered
NA037-026B	-2.27	-3.58		altered
NA037-026.1	-1.5	-3.81		altered
NA037-026.2	-2.84	-3.73		altered
Montserrat Eastside				
NA037-002A	2.06	2.78		marine
NA037-002B	2.32	-2.49		meteoric
NA037-002C	2.26	-2.71		meteoric
NA037-002.1	2.07	-3.64		meteoric
NA037-002.2	2.25	-3.02		meteoric
NA037-005A	2.07	1.82		marine
NA037-005B	2.05	1.86		marine
NA037-012A	2.19	1.06		marine
NA037-012B	2.46	1.09		marine
Montserrat Roche's Bluff				
RB 1	2.19	-8.43		hydrothermal
RB 2	2.21	-8.17		hydrothermal
RB 3	1.75	-6.97		hydrothermal
RB 4	2.09	-7.55		hydrothermal
Montserrat Geothermal Well-3				
950.1 m	2.21	-8.29		hydrothermal
950.2 m	1.97	-6.71		hydrothermal
950.4 m	1.99	-6.74		hydrothermal
950.3 m	2.16	-8.69		hydrothermal
2015.1 m	-0.93	-10.61		hydrothermal
2015.2 m	-0.57	-9.59		hydrothermal
2015.3 m	-0.65	-10.1		hydrothermal
2015.4 m	-0.83	-10.66		hydrothermal
2016.1 m	1.92	-11.21	shell	hydrothermal
2016.2 m	-3.71	-9.05		hydrothermal
2016.3 m	-2.81	-9.75		hydrothermal
Grenada Kick'em Jenny				
NA039-035	2.61	2.11		marine
NA039-071.1	-43.45	3.8		methanogenic
NA039-071.2	-40.42	3.58		methanogenic
Hellenic Arc, Kolumbo Seamount, Mediterranean				
NA007-001	3.17	2.93		marine
NA007-022	2.41	3.04		marine
NA007-045	1.89	2.8		marine

Also analysed for comparison: a coral sample from SW Montserrat nearshore (NA037-032.1, depth 182 m, dated at 12,000 yr), encrusting modern serpulids on sample NA037.032.2, modern bio-encrusters on sample NA037-033, C and D, and a large shell from Montserrat Well-3 depth 2016.1 m. The last column gives the interpretation of the data – see text for explanation.

Table 3. Sr isotope analyses of samples (with number of analyses in brackets) from Montserrat with the mean, minimum and maximum ages (95% confidence limits)

	Sample no.	$^{87}Sr/^{86}Sr$	MEAN (Ma)	min	max	likely interpretation
SW Nearshore						
	NA037-029 (2)	**0.709174**	**0.05**	0	0.15	original
	NA037-033 (3)	**0.709169**	**0.22**	0.18	0.25	original
SW Offshore						
	NA037-025 (2)	**0.709163**	**0.38**	0.33	0.42	original
	NA037-026 (4)	**0.708338**	**18.1**	18.03	18.18	altered
Eastside						
	NA037-002 (2)	**0.708166**	**24.65**	24.51	24.81	altered
	NA037-005 (2)	**0.70918**	**0**	0	0	original
	NA037-012 (2)	**0.709122**	**1.25**	1.23	1.28	original
Roche's Bluff						
	RBA-1,2,3 (3)	**0.708555**	**18.22**	18.15	18.3	altered
Geothermal well 3						
	2015 m (3)	**0.708568**	**18.07**	18.01	18.15	altered
	2016 m (3)	**0.708662**	**16.87**	16.82	16.92	altered
	1198 m (3)	**0.708779**	**15.15**	15.07	15.22	altered
	930.1 m (1)	**0.709158**	**0.52**	0.5	0.57	altered
	930.2 m (1)	**0.708792**	**14.85**	14.71	14.95	altered

Ages derived from the LOWESS 5 Fit spreadsheet, dated 26/03/13. See Howarth and McArthur (1997) for further information.
The last column gives the likely interpretation, whether the Sr signature records an original seawater value or an altered value through contact with hydrothermal fluid.